AD-A092 444 AIR FORCE INST OF TECH WRIGHT-PATTERSON AFB OH F/G 4/2
KINEMATIC FEATURES OF THE LARGE-SCALE MEAN STATE PHASE II OF GA--ETC(U)
AUG 80 R G HUGHES
UNCLASSIFIED AFIT-CI-80-39T NL

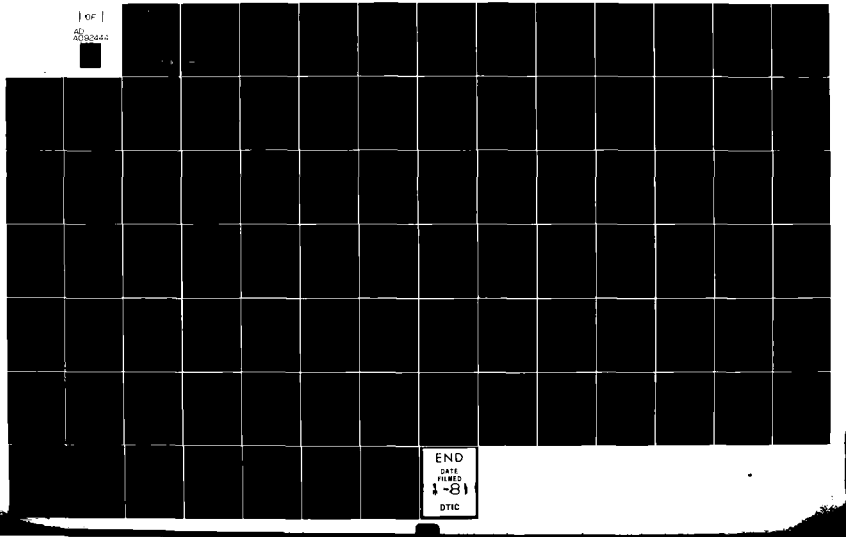

KINEMATIC FEATURES OF THE LARGE-SCALE MEAN STATE PHASE II OF GATE AND COMPARISON WITH PHASE III FEATURES

A Thesis

Submitted to the faculty

of

Purdue University

by

Robert Gordon Hughes

In Partial Fulfillment of the

Requirements for the Degree

of

Master of Science

August 1980

UNCLASS

SECURITY CLASSIFICATION OF THIS PAGE (When Data Entered)

REPORT DOCUMENTATION PAGE

READ INSTRUCTIONS BEFORE COMPLETING FORM

1 REPORT NUMBER: 80-39T	2 GOVT ACCESSION NO: AD-A093 444
3 RECIPIENT'S CATALOG NUMBER:	
4 TITLE (and Subtitle): Kinematic Features of the Large-Scale Mean State Phase II of Gate and Comparison with Phase III Features,	5 TYPE OF REPORT & PERIOD COVERED: THESIS/DISSERTATION/
	6 PERFORMING ORG. REPORT NUMBER:
7 AUTHOR(s): Robert Gordon Hughes	8 CONTRACT OR GRANT NUMBER(s):
9 PERFORMING ORGANIZATION NAME AND ADDRESS: AFIT STUDENT AT: Purdue University	10 PROGRAM ELEMENT PROJECT, TASK AREA & WORK UNIT NUMBERS:
11 CONTROLLING OFFICE NAME AND ADDRESS: AFIT/NR WPAFB OH 45433	12 REPORT DATE: August 1980
	13 NUMBER OF PAGES: 76
14 MONITORING AGENCY NAME & ADDRESS (if different from Controlling Office): 14 AFIT-SI-80-39T	15 SECURITY CLASS. (of this report): UNCLASS
	15a DECLASSIFICATION DOWNGRADING SCHEDULE:

16 DISTRIBUTION STATEMENT (of this Report)

APPROVED FOR PUBLIC RELEASE; DISTRIBUTION UNLIMITED

Accession For	
NTIS GRA&I	X
DTIC TAB	☐
Unannounced	☐
Justification	
By	
Distribution/	
Availability Codes	
Dist	Avail and/or Special
A	

17 DISTRIBUTION STATEMENT (of the abstract entered in Block 20, if different from Report)

18 SUPPLEMENTARY NOTES

APPROVED FOR PUBLIC RELEASE: IAW AFR 190-17

Air Force Institute of Technology (ATC)
Wright-Patterson AFB, OH 45433

Fredric C. Lynch

FREDRIC C. LYNCH, Major, USAF
Director of Public Affairs

19 KEY WORDS (Continue on reverse side if necessary and identify by block number)

20 ABSTRACT (Continue on reverse side if necessary and identify by block number)

[redacted]

DD FORM 1 JAN 73 1473 EDITION OF 1 NOV 65 IS OBSOLETE

UNCLASS

SECURITY CLASSIFICATION OF THIS PAGE (When Data Entered)

AFIT RESEARCH ASSESSMENT

The purpose of this questionnaire is to ascertain the value and/or contribution of research accomplished by students or faculty of the Air Force Institute of Technology (ATC). It would be greatly appreciated if you would complete the following questionnaire and return it to:

AFIT/NR
Wright-Patterson AFB OH 45433

Research Title: Kinematic Features of the Large-Scale Mean State Phase II of Gate and Comparison with Phase III Features

Author: Robert Gordon Hughes

Research Assessment Questions:

1. Did this research contribute to a current Air Force project?

   a. Yes b. No

2. Do you believe this research topic is significant enough that it would have been researched (or contracted) by your organization or another agency if AFIT had not?

   a. Yes b. No

3. The benefits of AFIT research can often be expressed by the equivalent value that your agency achieved/received by virtue of AFIT performing the research. Can you estimate what this research would have cost if it had been accomplished under contract or if it had been done in-house in terms of manpower and/or dollars?

   a. Man-years _____. b. $_____

4. Often it is not possible to attach equivalent dollar values to research, although the results of the research may, in fact, be important. Whether or not you were able to establish an equivalent value for this research (3 above), what is your estimate of its significance?

   a. Highly Significant b. Significant c. Slightly Significant d. Of No Significance

5. AFIT welcomes any further comments you may have on the above questions, or any additional details concerning the current application, future potential, or other value of this research. Please use the back of this questionnaire for your statement(s).

NAME GRADE POSITION

ORGANIZATION LOCATION

USAF SCN 75-20B

To my wife Susan who will never

take a back seat again.

ACKNOWLEDGMENTS

I wish to extend my gratitide to Dr. Dayton G. Vincent who proposed this undertaking and was always available for encouragement and expertise when it was needed. The patience and tolerance which he displayed are truly appreciated. Special thanks go to Dr. Phillip J. Smith and Dr. Ernest M. Agee for their critical review of this text and probing questions which, in the end, lent much to its content.

I am grateful to the United States Air Force and the Air Force Institute of Technology for making this opportunity possible.

I am thankful to Gregory L. Scott and Huo-Jin Huang for their delightful and enlightening discussion on results, techniques and programming problems and to Mr. Randy Peppler for his excellent drafting work.

Last, but certainly not least, I am eternally grateful to my wife, Susan, who stood beside me and occasionally behind me pushing when necessary to keep me moving. She helped me maintain my composure when things got rough and helped me laugh when things got bleak.

TABLE OF CONTENTS

	Page
LIST OF TABLES	v
LIST OF FIGURES	vi
ABSTRACT	viii
CHAPTER 1. INTRODUCTION	1
CHAPTER 2. COMPUTATIONAL PROCEDURES	14
2.1 Data Processing	14
2.2 Computed Quantities	15
CHAPTER 3. RESULTS	19
3.1 Horizontal Motion	20
3.2 Horizontal Divergence	34
3.3 Vertical Motion	43
3.4 Relative Vorticity	49
3.5 Vorticity Budget	58
CHAPTER 4. CONCLUSIONS	68
REFERENCES	72
APPENDIX	76

LIST OF TABLES

Table Page

1. GATE Operations Schedule (after Kuettner, 1974)... 3

LIST OF FIGURES

Figure		Page
1.	Gate A-scale area	6
2.	Wind data network for Phase II analysis region	8
3.	Study area with water and land subregions	10
4.	Streamline and isotachs in m s^{-1} for Phase II at surface, 700 mb and 200 mb	22
5.	Cross-section of zonal wind (u) in m s^{-1} and temporal standard deviation of zonal wind (σu) along 16°N and 6°N	25
6.	Cross-section of zonal wind (u) in m s^{-1} for Phase II along 24°W and 4°W	28
7.	As in Figure 6, except for meridional wind	31
8.	Vertical distribution of area averages for zonal wind (u) and meridional wind (v) in m s^{-1} for subregion shown in Figure 2	33
9.	Horizontal divergence ($\nabla_p \cdot \vec{V}$) in $10^{-6}s^{-1}$ for Phase II for surface-850 mb and 250-200 mb layers	36
10.	Cross-sections of horizontal divergence ($\nabla_p \cdot \vec{V}$) in $10^{-6}s^{-1}$, vertical motion (ω) in 10^{p_3} mb s^{-1}, and relative vorticity (ζ) in $10^{-5}s^{-1}$ for Phase II along 13°N	39
11.	As in Figure 8, except for horizontal divergence ($\nabla_p \cdot \vec{V}$) in $10^{-6}s^{-1}$, vertical motion (ω) in 10^{-3} mb s^{-1}, and relative vorticity (ζ) in $10^{-5}s^{-1}$	42

Figure Page

12. Vertical motion (ω) in 10^{-3} mb s^{-1} for Phase II at 700 mb, 500 mb, and 200 mb..... 45

13. As in Figure 6, except for vertical motion in 10^{-3} mb s^{-1}..... 48

14. Relative vorticity (ζ) in $10^{-5}s^{-1}$ for Phase II at 850 mb, 700 mb and 200 mb..... 51

15. As in Figure 6, except for relative vorticity in $10^{-5}s^{-1}$..... 54

16. Vertical shear of relative vorticity ($\zeta_{850}-\zeta_{200}$) in $10^{-5}s^{-1}$..... 57

17. Cross-section of meridional gradient of absolute vorticity averaged for water and land subregions in 10^{-13} s^{-1} m^{-1}..... 60

18. As in Figure 6, except for vorticity budget terms in $10^{-11}s^{-1}$, see text for details..... 62

ABSTRACT

Hughes, Robert Gordon. M.S., Purdue University, August, 1980. KINEMATIC FEATURES OF THE LARGE-SCALE MEAN STATE PHASE II OF GATE AND COMPARISON WITH PHASE III FEATURES. Major Professor: Dayton G. Vincent.

Large-scale wind field features are presented for Phase II of the Global Atmospheric Research Program's (GARP) Atlantic Tropical Experiment (GATE) and compared with those of Phase III. GATE took place over western Africa and the tropical eastern Atlantic in 1974. Phase II was from 28 July to 17 August and Phase III was from 30 August to 19 September. The Final Validated Data Set (FVDS), consisting of 21 day time-averaged values for station data at mandatory reporting levels from the surface to 100 mb, was subjectively analyzed.

Presented here are streamline and isotach analyses, derived horizontal winds, kinematic vertical motion, horizontal divergence, and vorticity including the vorticity budget terms. During Phase II, low-level circulation was dominated by convergence and cyclonic vorticity over land; however, over water, divergence dominated. This result and the related patterns of vertical motion seem to be a major difference between circulation features of Phase II and Phase III.

Many investigators note that with regard to cloudiness, convection, rainfall, and wave organization and structure, Phase III was more active than Phase II. Comparisons of the analyzed and derived wind data and kinematic variables from this study and that of Vincent and Scott (1980) are made in an attempt to relate these differences in activity to the above findings.

CHAPTER 1

INTRODUCTION

The tropics occupy a large portion of the earth's surface and its atmosphere. Furthermore, this portion of the globe plays an important role in the energy balance and general circulation of the planet. For this reason, it is essential that information regarding tropical weather systems and climate be obtained. The quality and quantity of observations in tropical regions have recently increased dramatically through the use of both polar orbiting and geostationary satellites. Unfortunately, however, most of the tropical surface area is either ocean, uninhabited deserts or forests, where routine observations are not available. In addition, upper tropospheric data is not always reliable.

In 1966 an important event with regard to tropical weather and climate was initiated, the Global Atmospheric Research Program (GARP). It commenced through the combined efforts of the United Nations, the World Meteorological Organization (WMO), the International Council of Scientific Unions (ICSU) and the United States National Academy of Sciences. Essentially the two basic objectives of GARP are to:

1. increase the accuracy of forecasts over periods from one day to several weeks through the study of large-scale fluctuations which control changes in the weather and

2. understand the factors that determine the statistical properties of the general circulation, thus leading to a better understanding of the physical basis of climate.

During the early planning of GARP, it was recognized that there existed a need for detailed studies in the tropics (GATE Report No. 1, 1972). Specialized subprograms such as the Barbados Oceanographic Meteorological Experiment, 1969 (BOMEX), GARP Atlantic Tropical Experiment, 1974 (GATE) and the Monsoon Experiment, 1979 (MONEX) have aided in the effort to increase our knowledge and understanding of meteorological processes in the tropics and their contribution to global circulations.

Of particular interest to the present thesis is the GATE experiment. This was a major field program which took place from June 19 to September 23 of 1974. As a subprogram of GARP, it attempted to satisfy the major objectives of GARP. Additionally, GATE's major objectives (GATE Report No. 3, 1974) were as follows:

1. to provide a means of estimating the effect of smaller scale tropical systems on the large-scale (synoptic-scale) circulation and

2. to facilitate the development of numerical modelling and prediction techniques.

The GATE field program consisted of three observational periods (Table 1). The observed area included

Table 1. GATE Operations Schedule (after Kuettner, 1974).

DATE		EVENT
From	To	
19 June	25 June	Enroute, intercomparison
26 June	16 July	Phase I observation (21 days)
17 July	27 July	Enroute, intercomparison
28 July	17 August	Phase II observation (21 days)
18 August	29 August	Enroute, intercomparison
30 August	19 September	Phase III observation (21 days)
20 September	23 September	Enroute, intercomparison

portions of Africa, the Atlantic Ocean and the Carribbean Sea (Figure 1). During these periods, the upper air network, especially over the ocean area, was increased through the addition of over 40 research ships. In addition, there were increased observations from existing land and island stations as well as numerous flights by meteorologically equipped aircraft. This amounted to increasing the existing network nearly by a factor of three (Kuettner, 1974).

The present study investigates the mean flow features and kinematic properties of Phase II (28 July to 17 August) and compares these features with those of Phase III (30 August to 19 September). The area of interest is bounded by 20°N, 10°E, 10°S and 40°W, a subportion of the GATE A-scale (Figure 2). The variables analyzed are wind direction (β) and wind speed ($|\vec{V}|$), zonal wind (u), meridional wind (v), and the temporal standard deviations of the u and v components (σ_u, σ_v). The kinematic quantities derived and analyzed are horizontal divergence ($\nabla_p \cdot \vec{V}$), relative and absolute vorticity (ζ, ζ_a), and the vertical motion (ω). Vertical distributions of area averages of u, v, the above-named kinematic quantities, and terms in the vorticity budget are presented for a region bounded by 18°N, 4°N, 8°E, and 38°W (Figure 3), where the data density is greatest. Furthermore, the latter results are partitioned into a land subregion, 15°W, 8°E, 18°N, 4°W, and a water region, 38°W, 15°W, 18°N, 4°N, so that

Figure 1. Gate A-scale area.

GATE A-SCALE AREA

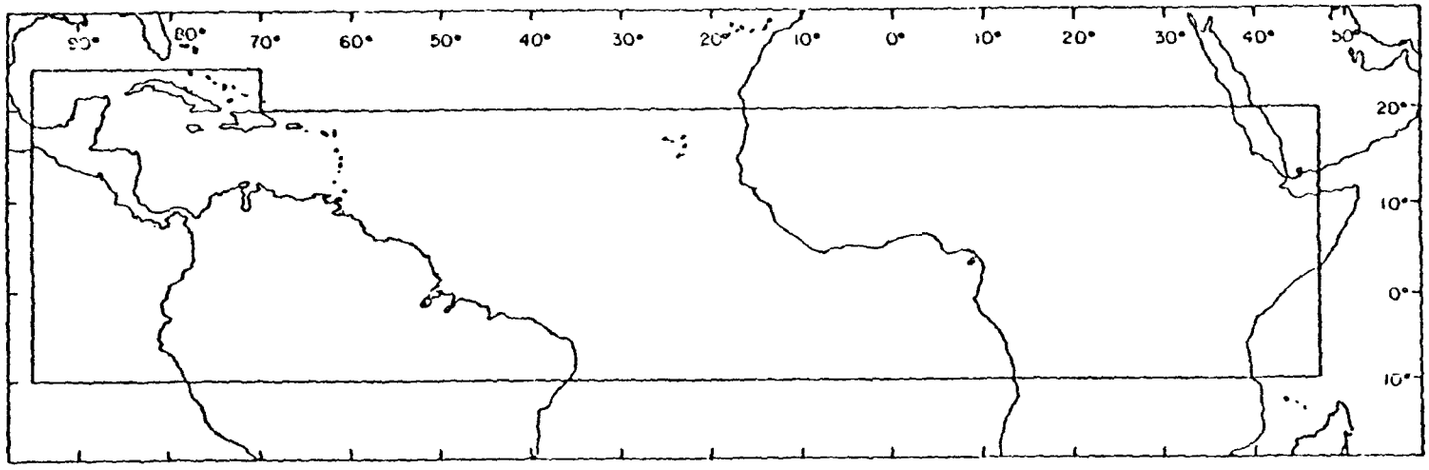

Figure 1

Figure 2. Wind data network for Phase II analysis region. Dots indicate stations where observations do not extend above 700 mb.

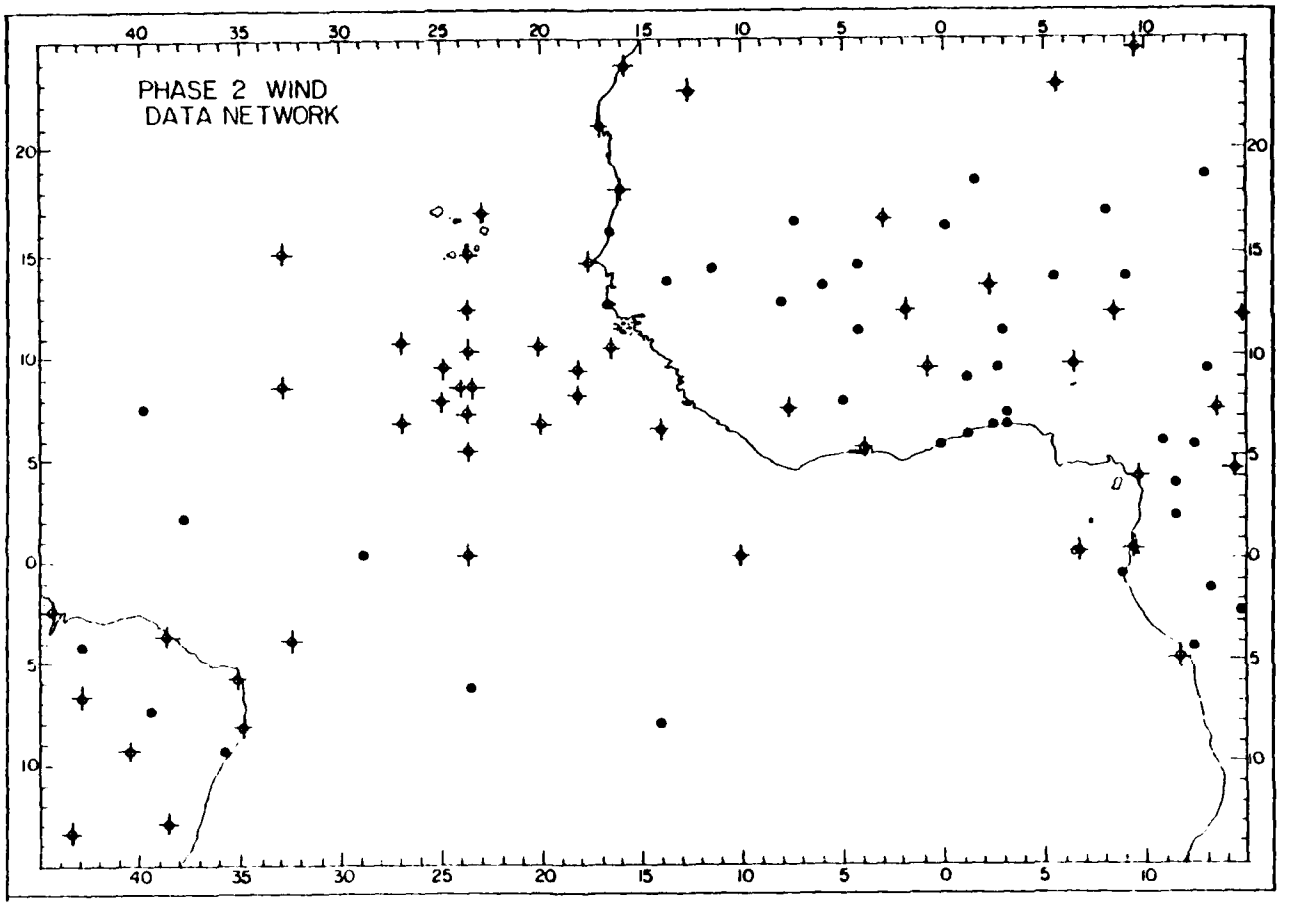
PHASE 2 WIND
DATA NETWORK
40
35
30
25
20
15
10
5
0
5
10
20
15
10
5
0
5
10

Figure 2

Figure 3. Study area with water and land subregions.

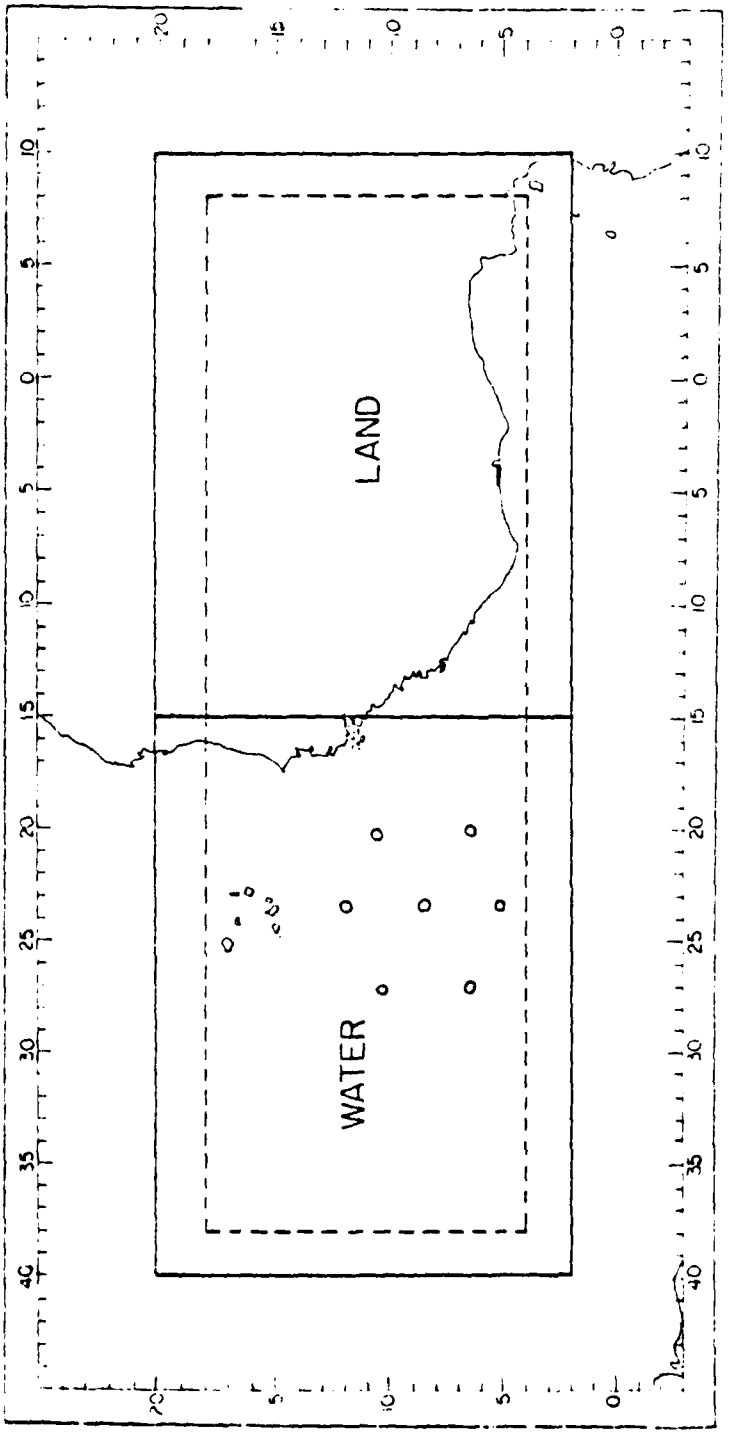

Figure 3

differences in these two areas can be examined. Calculations of Phase II variables are made and compared with similar results for Phase III reported by Vincent (1980) and Vincent and Scott (1980), as well as other investigators of Phase II mean state data.

Prior to and since GATE a number of investigators have examined the mean state and wave-like properties of the GATE region. Burpee (1972) studied the origin and structure of easterly waves over north Africa. He concluded that these waves generally form over central north Africa and are directly linked to the mid-tropospheric jet located in the baroclinic zone just south of the Sahara Desert. Carlson (1969) produced streamline and isotach analyses for July, August and September 1968 showing that waves move over west Africa in a continuous wave train, intensifying as they approach the West African cost. Aspliden (1974) showed that semi-permanent cyclonic features appear in the mean flow over Africa in the lower troposphere. He notes that the appearance of "West African disturbance lines" may be related to the low level waves associated with a trough axis line extending through the northern African region. Frank (1969) using satellite data, suggests that "inverted V" cloud signatures are often associated with these easterly waves and can be tracked westward into the eastern Pacific. Sadler (1975) averaged seven years of satellite and ten years of commercial aircraft data, as well as other data, to obtain a time-mean average for the

flow pattern and cloudiness over the GATE area for the layer from 27,000 to 41,000 feet.

More recently, investigations based on GATE data have begun to appear in the literature. Nearly all of these studies rely on the use of Phase III data. Many of these investigations focus on analyses of composite tropical wave disturbances (e.g., Reed et al., 1977; Shapiro, 1978; Stevens, 1979; and Thompson et al., 1979). Some of these investigations also included mean state analyses of one or more variables from Phase III data. Reed et al. (1977) used the Quick Look Data Set (QLDS) to analyze mean zonal wind, temperature deviation, relative humidity and absolute vorticity. Viltard and deFelice (1979) used spectral analysis for all three phases of GATE and looked at wind speeds in an easterly wave over Africa.

To date, most work on time-mean variables of Phase II has appeared in atlases such as those produced by Depradine et al. (1978), 300 mb; Krishnamurti et al. (1978), 200 mb; and Pasch et al. (1978), 250 mb. Gray et al. (1976) averaged five years of data (1968-1972), and presented monthly averages of u, v, stream function and wind speed for several levels for the area 50°N to 50°S and 90°W to 110°E. In addition, Tourre et al. (1979) objectively analyzed mean streamlines and isotachs for six levels in the atmosphere and calculated mean divergence and relative vorticity at these levels. Estoque and Douglas (1978) discussed causal mechanisms for ITCZ placement using Phase

II data. Sadler and Oda (1979) subjectively analyzed surface and 250 mb winds for Phase II to produce daily maps of streamlines and isotachs.

Studies of Phase II data have in the past been restricted to either a small number of variables, limited layers in the atmosphere, or have utilized objective analysis techniques. This thesis attempts to analyze, for the mean state, several kinematic variables at all standard levels using subjective analysis techniques, and further attempts to differentiate features in the kinematic analysis between land and water areas. The primary objectives of this thesis are to: (1) illustrate and discuss the flow features of Phase II, including analyses of wind direction and speed, horizontal divergence, absolute and relative vorticity and vertical (p) velocity for time-averaged mean state of the region shown in Figure 2; (2) composite the area-averaged vertical distributions of these variables, as well as that of the vorticity budget; (3) present differences in these distributions over land and water; (4) relate properties of the mean state to barotropic instability processes; and (5) examine differences between Phase II and Phase III mean state.

CHAPTER 2

COMPUTATIONAL PROCEDURES

2.1 Data Processing

During GATE there was an increase not only in the number of rawinsonde stations, but also in the frequency of reports. Observations were taken, in some cases, every six hours at approximately 0000 GMT, 0600 GMT, 1200 GMT and 1800 GMT. These data were archived and validated at the Dynamic Climatology branch of the British Meteorological Office, Bracknell, United Kingdom, as part of their role as coordinator for the GATE synoptic-scale subprogramme. Messrs. Paul Graystone, the director, and Steve Farmer, programmer, were responsible for supplying the data used in the present study.

These data were the time-mean values for each station taken from the Final Validated Data Set (FVDS) provided by the Meteorological Office. Many of the stations did not have the same number of observations for each reporting time. In order to obtain an overall average, the data for each reporting time were averaged over the entire observational phase, using the number of observations as a weighting factor.

Subjective analyses of the variables and computed quantities discussed in Chapter 1 were performed at the surface, 850 mb, 700 mb, 500 mb, 400 mb, 300 mb, 250 mb, 200 mb, 150 mb and 100 mb. A two degree latitude/longitude grid was used to extract grid point values over the area from 40°W to 10°E and 10°S to 20°N (Figure 3). The gridded data were objectively analyzed using a plotting routine supplied by the National Center for Atmospheric Research (NCAR). This made it possible to identify errors in the data that may have occurred in the data reduction process. Analyses were also checked for vertical continuity.

2.2 Computed Quantities

All computed quantities were calculated using this final gridded data set. In calculating these quantities, spherical coordinates and centered finite-difference techniques were employed.

Horizontal divergence was calculated from

$$\nabla_p \cdot \vec{V} = \frac{\partial u}{\partial x} + \frac{\partial v}{\partial y} - v \frac{\tan\phi}{a} \qquad (1)$$

where a is the radius of the earth and ϕ is latitude.

Vertical velocities (ω) were calculated by the kinematic method, integrating the equation of continuity in isobaric coordinates

$$\nabla_p \cdot \vec{V} = - \frac{\partial w}{\partial p} \qquad (2)$$

to obtain

$$\omega_u = \omega_\ell + \int_{P_u}^{P_\ell} \nabla_p \cdot \vec{V} \, dp \qquad (3)$$

where

ω_u = at the upper level,

ω_ℓ = at the lower level,

p_u = p at the upper level,

p_ℓ = p at the lower level.

The primary advantage of the kinematic method is in the simplicity of (3), where the only equation is that of hydrostatic balance. In the present study, the scales of motion of the tropical mean state validate the use of this assumption. One of the shortcomings of the kinematic method (Smith, 1970) is that, in its formulation, the vertical velocity at any given level depends not only upon the accuracy of divergence in that layer, but also on the integrated horizontal divergence in the layers below it. Consequently, errors in vertical motion are subject to this cumulative bias effect and will increase with height.

The problem of cumulative bias error can be compensated for by a suitable correction scheme. In the present study, a scheme developed by O'Brien (1970), for the special case when the error variance is a linear function of pressure was applied. This technique assumes no net mass divergence in the column of air from the surface to the top of the atmosphere (100 mb for this case). Hence,

it requires that $\omega = 0$ at the surface and at 100 mb. This technique, applied to the kinematic method, has been reviewed by Smith (1970) and found compatible for mid-latitude systems. It has also been successfully applied by several investigators using tropical data (e.g., Vincent and Waterman, 1979; Vincent and Scott, 1980).

Relative vorticity (ζ) was computed in spherical coordinates from

$$\zeta = \frac{\partial v}{\partial x} - \frac{\partial u}{\partial y} + \frac{u\tan\phi}{a} \tag{4}$$

To obtain the absolute vorticity (ζ_a), the planetary vorticity $2\Omega\sin\phi$ (f) was added to the relative vorticity in (4), where Ω represents the angular velocity of the earth.

The vorticity equation in isobaric coordinates can be written as follows

$$\frac{\partial \zeta}{\partial t} = -\vec{V} \cdot \nabla_p \zeta_a - \omega \frac{\partial \zeta}{\partial p} - \zeta_a \nabla_p \cdot \vec{V} + \frac{\partial \omega}{\partial y}\frac{\partial u}{\partial p}$$

$$- \frac{\partial \omega}{\partial x}\frac{\partial v}{\partial p} + \frac{\partial F_x}{\partial y}\frac{\partial F_y}{\partial x} \tag{5}$$

In order to apply the present mean state data to (5), it is necessary to partition the variables into mean and eddy components. Pertubation theory suggests that

$$\textcircled{H} = \overline{\textcircled{H}} + \textcircled{H}' \tag{6}$$

where $\overline{(H)}$ represents the time mean state component

$(H)'$ represents the departure (eddy) from the time mean.

Applying this to (5) yields

$$\underbrace{\frac{\partial \zeta_a}{\partial t}}_{0} = \underbrace{-\bar{V}\cdot\nabla_p \bar{\zeta}_a}_{\text{HADV}} \underbrace{-\bar{\omega}\frac{\partial \bar{\zeta}}{\partial p}}_{\text{VADV}} \underbrace{-\bar{\zeta}_a \nabla_p \cdot \bar{V}}_{\text{DIV}} \underbrace{+\frac{\partial \bar{\omega}\partial \bar{u}}{\partial y \partial p} - \frac{\partial \bar{\omega}\partial \bar{v}}{\partial x \partial p}}_{\text{TILT}} \tag{7}$$

$$+ \underbrace{\frac{\partial F_x}{\partial y} - \frac{\partial F_y}{\partial x} - \overline{V'\cdot\nabla_p \zeta_a'} - \overline{\omega' \frac{\partial \zeta}{\partial p}'} - \overline{\zeta_a' \nabla_p \cdot V'} + \overline{\frac{\partial \omega' \partial u'}{\partial y \partial p}} - \overline{\frac{\partial \omega' \partial v'}{\partial x \partial p}}}_{\text{RES}}$$

In the present study, HADV, VADV, DIV and TILT were calculated from grid point data. Hence, the residual (RES) represents all terms in (5) not calculated and is essentially an imbalance of the calculated terms. Effects which contribute to the value of RES include, time-departure effects due to synoptic-scale transient waves mean state frictional effects and errors in the other terms in the equation. The vertical advection term (VADV) and the tilting term (TILT), utilize the mean corrected vertical motion for the layer in the calculation of $\partial\omega/\partial p$. The divergence term (DIV) was calculated using the adjusted vertical motion substituted from (2) in place of $\nabla_p \cdot \vec{V}$.

CHAPTER 3

RESULTS

Some of the results will involve area averages taken over the whole latitude band as well as the land and water subareas, described in Chapter 2. The separation of results into land and water subareas stems from analyses of other investigators (e.g., Reed et al., 1977), who examined differences in the wave structure and noted that, while wave characteristics were similar for both land and water, " . . . some differences were observed, however, which are believed to be real.".

Cross-sectional analyses of horizontal motions (u, v), vertical motion (ω), relative vorticity (ζ), and absolute vorticity (ζ_a) are presented along 24°W and 4°W for intercomparison between water and land and for comparison with Phase III results given by Vincent (1980) and Vincent and Scott (1980).

Horizontal map analyses for ω, ζ, u, v, temporal standard deviation of the zonal wind (σu), vorticity shear ($\zeta_{850} - \zeta_{200}$) and divergence ($\nabla_p \cdot \vec{V}$) are discussed in an effort to describe the mean state and to identify preferential areas for enhancement or diminution of easterly waves traveling across Africa and into the eastern Atlantic.

Reed et al. (1977) suggests that waves were better organized and more uniform in Phase III than in the previous phases. Frank (1975) and Sadler and Oda (1979) both agree. Nicholson (1975) suggests that during Phase III convection was more intense and wide spread than during Phase II. Vertical distributions of area averages of u, v, $\nabla_p \cdot \vec{V}$, ζ and the vorticity budget terms over land and water are examined and compared to Phase III in an effort to identify possible causal mechanisms which would contribute to the differences in mean state and wave activity between phases. Also shown are cross-sections of the meridional gradient of absolute vorticity averaged over the land and water subregions to examine the condition for barotropic instability.

3.1 Horizontal Motion

Figure 4 shows streamline and isotach analyses at the surface, 700 mb and 200 mb. Comparison of these flow fields with those of climatological studies (e.g., Newell et al., 1972; Gray et al., 1976) indicate that, within one standard deviation, Phase II mean state wind variables were typical. When compared to Phase III, distributions also are in agreement. Salient features include the surface col near 3°W, 8°N. This position is south and west of the 50 year August mean of 29°W, 11°N (Aspliden et al., 1976). The confluence zone extending eastward and northward from this col is 1° to 2° south of its 50 year August average

Figure 4. Streamline and isotachs in m s^{-1} for Phase II at surface, 700 mb and 200 mb.

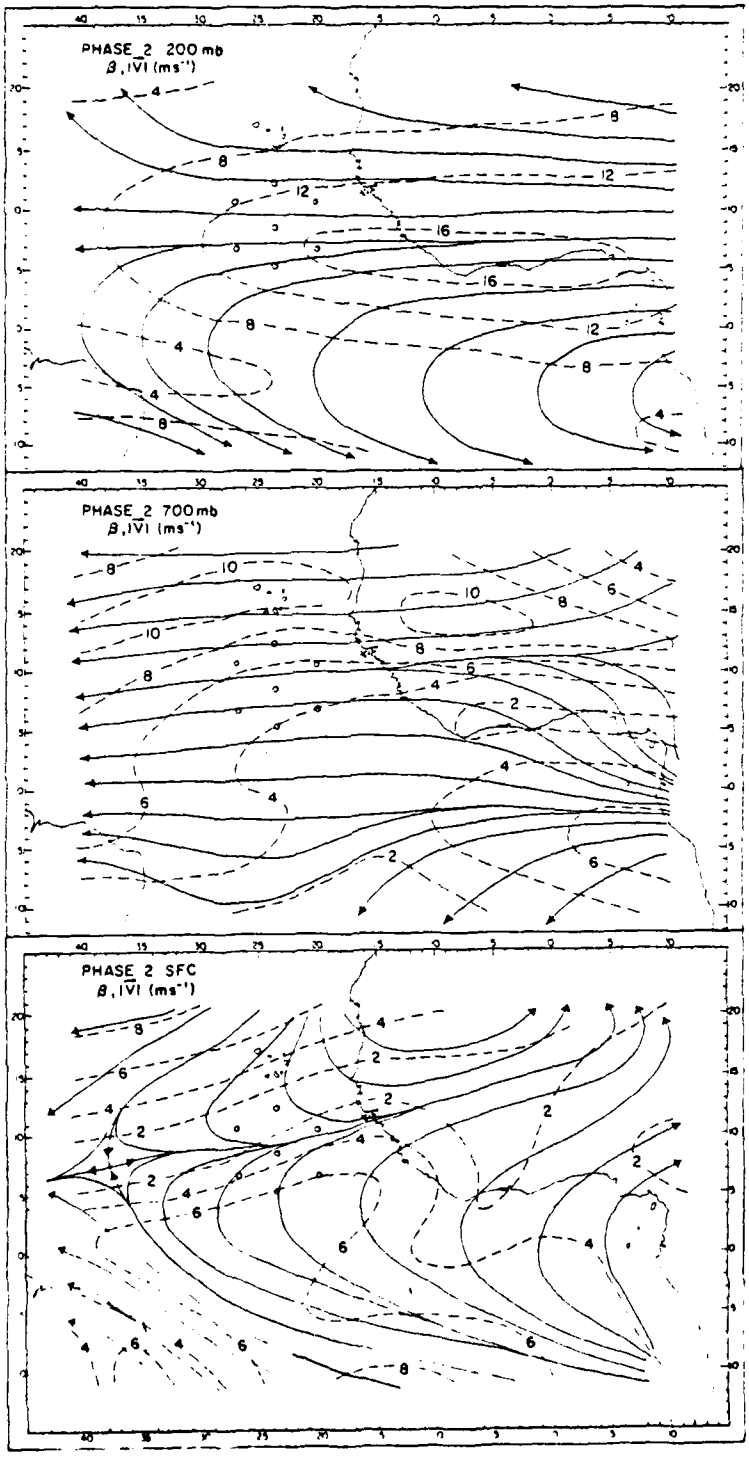

Figure 4

(loc cit.) and about 3° west of its Phase III position. Also evident is the southwest monsoon circulation over Africa which dominates this region during northern summer. The westerlies over northern Africa represent the flow around the heat low over the Sahara Desert.

The flow at 700 mb reveals that the mid-tropospheric jet or African Easterly Jet is located at about 15°N over land and 17°N over water. The confluence line over land near 10°N is well documented by Newell et al. (1972). During Phase III the mid-tropospheric jet shifts southward to 13°N over land and 15°N over water while the confluence line at 700 mb shifts southward to 5°N and diminishes in strength. The 700 mb level is where the westerly propagating waves are most pronounced. The upper level jet, as depicted in the 200 mb analysis, is located near 6°N. The difluence line near 8°N is also well documented by Newell et al. (1972). Upper level flow (200 mb) during Phase III was similar to Phase II in both magnitude and direction. However, during Phase III average placement of the wind maximum was at 4°N.

Figure 5 represents the vertical distribution of zonal wind and its temporal standard variation along the average axis of the mid-tropospheric and upper tropospheric jets, 16°N and 6°N, respectively. The dominant feature of the mid-tropospheric jet is its extension over the eastern Atlantic. While its existence over the continent has long been known, this extension over water was not known prior

Figure 5. Cross-section of zonal wind(u) in m s^{-1} and temporal standard deviation of zonal wind (σu) along 16°N and 6°N.

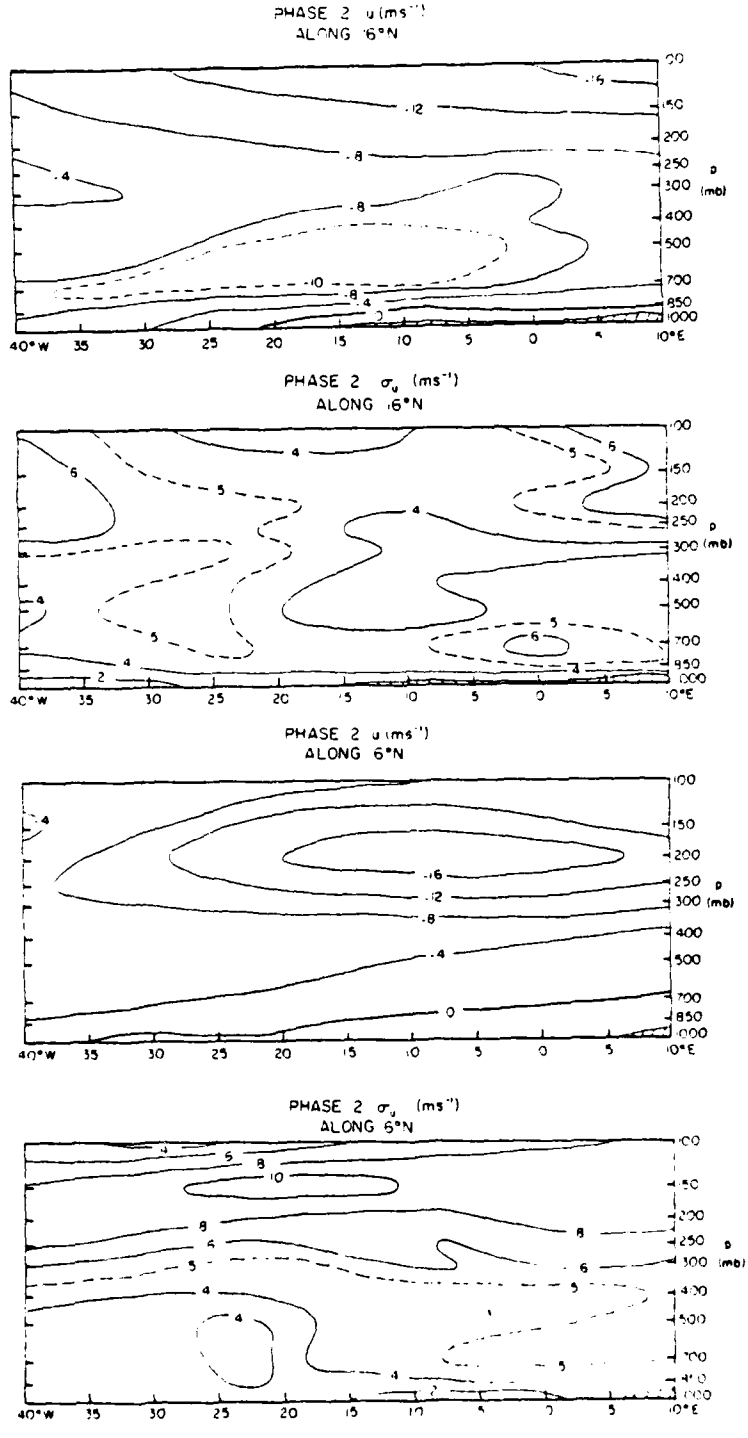
PHASE 2 u (ms⁻¹)
ALONG 6°N
PHASE 2 σu (ms⁻¹)
ALONG 6°N
PHASE 2 u (ms⁻¹)
ALONG 6°N
PHASE 2 σu (ms⁻¹)
ALONG 6°N
p (mb)
40°W
35
30
25
20
15
10
5
0
5
10°E

Figure 5

to GATE. A possible reason for the extension over water is the continuation of the north-south temperature gradient from Africa into the eastern Atlantic. Carlson and Benjamin (1980) suggest that this is due to the advection of dust from the Sahara Desert by the low-to-mid level easterly flow and the resultant warming of the air over the eastern Atlantic by solar absorption. This extension was also documented by Burpee and Dugdale (1975) for all three phases and by Vincent (1980) for Phase III. The diminution of the vertical extent of the mid-tropospheric jet is evidence of the weakening effect of this heating of the dust due to dispersal.

The largest standard variations of u (σu) occur in the vicinity of each jet. This variability in the mid-tropospheric jet is associated with westward propagating wave disturbances. In the upper troposphere, an examination of daily 250 mb streamline and isotach maps for Phase II (Sadler and Oda, 1979) suggests that variations are due to both latitudinal and speed variations of the jet.

Figure 6 shows the zonal wind component along 24°W and 4°W. The main features of the zonal flow are the mid-tropospheric and upper tropospheric jets, previously discussed. Wind speeds for the mid-tropospheric jet were weaker in Phase II than in Phase III; whereas, the upper level jets were about the same strength in both phases. As noted earlier, the positions of the mid-tropospheric

Figure 6. Cross-section of zonal wind (u) in m s^{-1} for Phase II along 24°W and 4°W.

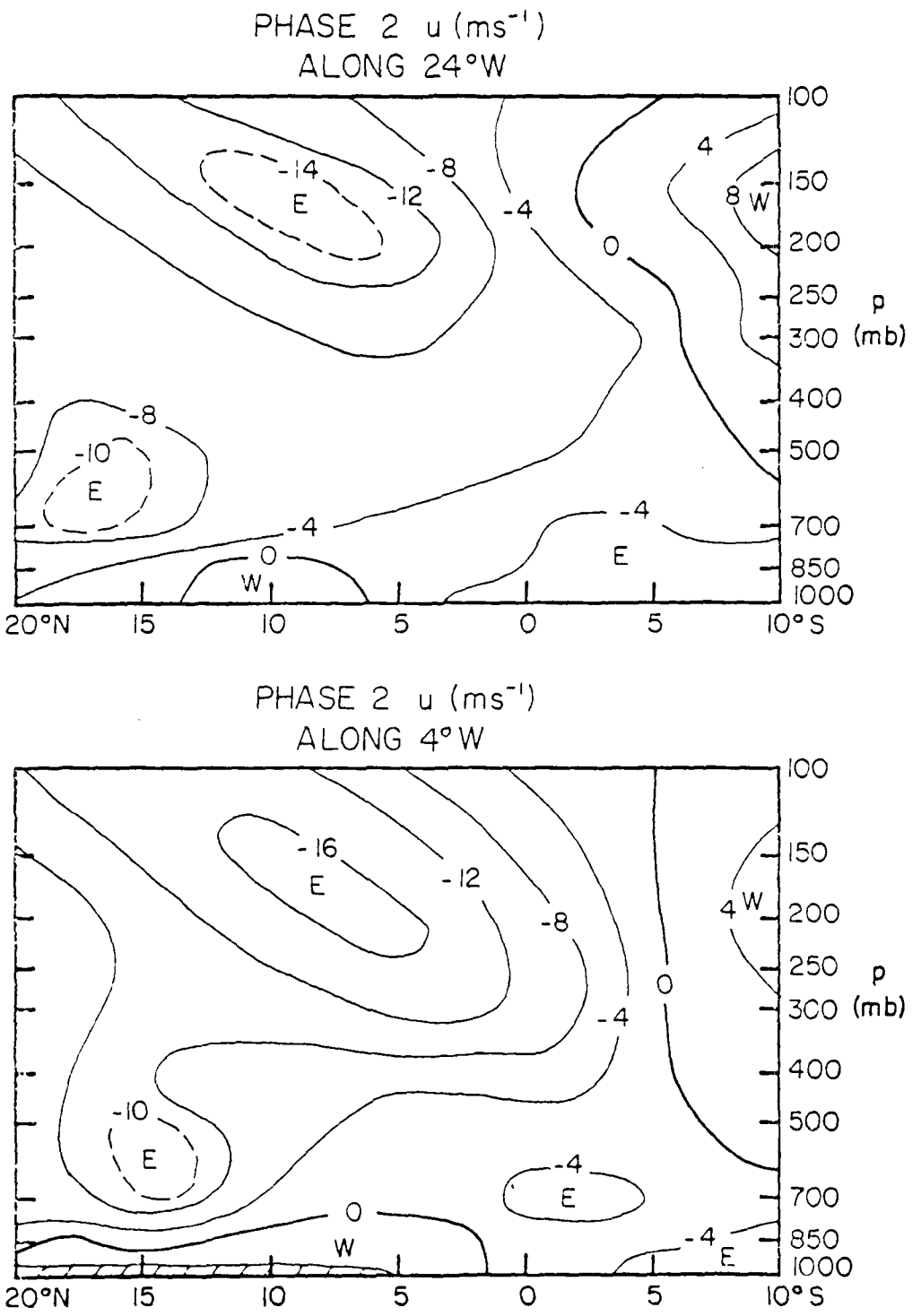
PHASE 2 u (ms⁻¹)
ALONG 24°W
-14
E
-12
-8
-4
0
4
8 W
-8
-10
E
-4
0
W
-4
E
100
150
200
250
300
400
500
700
850
1000
p
(mb)
20°N
15
10
5
0
5
10°S
PHASE 2 u (ms⁻¹)
ALONG 4°W
-16
E
-12
-8
-4
0
4 W
-10
E
-4
E
0
W
-4
E
100
150
200
250
300
400
500
700
850
1000
p
(mb)
20°N
15
10
5
0
5
10°S

Figure 6

and upper tropospheric jets are about 2° north of their Phase II positions. The low level westerlies which occur over land are associated with the southwest monsoon circulation and the flow around the Sahara heat low. The northward shift in the mid-tropospheric jet location from land to water is due to the northward shift of the maximum of the low level temperature gradient.

Figure 7 shows the meridional wind component over land and water. The low level convergence of this component is easily identifiable over water; however, the low level extension of the southwest monsoon over land makes convergence less discernible over land. The upper level divergence is easily seen over both land and water.

Figure 8 represents the vertical profile of area-averaged values of both u and v over the land and water subareas, as well as over the whole area. Easterly flow dominates above the surface, maximizing near 150 mb. This is in good agreement with Phase III (Scott, 1980). Over land at low levels, westerlies associated with the monsoon circulation dominate. Low level southerly flow over land is also attributable to the monsoon circulation. Above 300 mb, southerly flow associated with the anticyclonic flow north of the upper tropospheric jet dominates over both land and water, maximizing near 150 mb.

Figure 7. As in Figure 6, except for meridional wind.

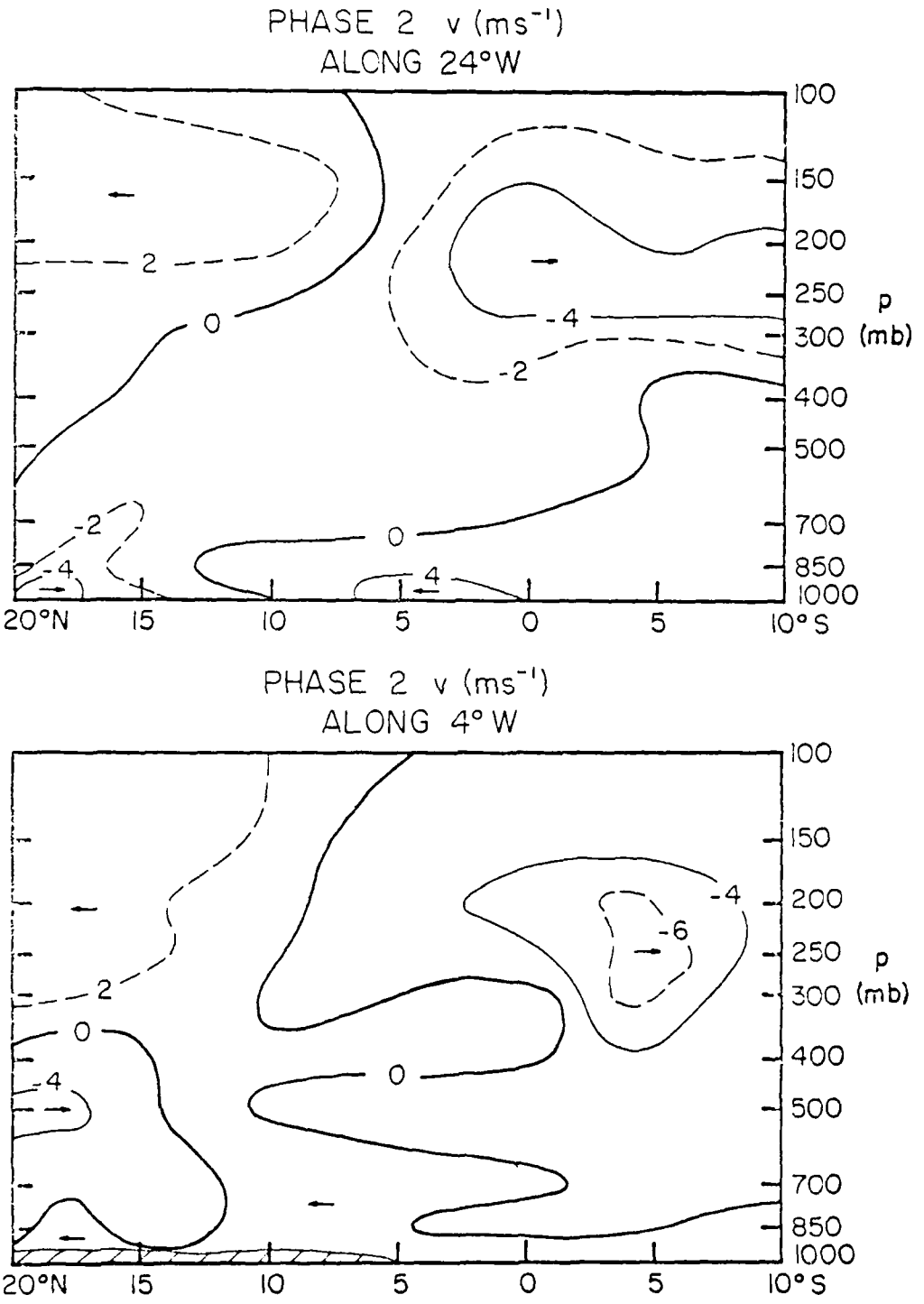
PHASE 2 v (ms⁻¹)
ALONG 24°W
100
150
200
250
300
400
500
700
850
1000
p
(mb)
2
0
-2
-4
-4
-2
0
4
20°N
15
10
5
0
5
10°S
PHASE 2 v (ms⁻¹)
ALONG 4° W
100
150
200
250
300
400
500
700
850
1000
p
(mb)
-4
-6
2
0
-4
0
20°N
15
10
5
0
5
10°S

Figure 7

Figure 8. Vertical distribution of area averages for zonal wind (u) and meridional wind (v) in m s^{-1} for subregion shown in Figure 3.

PHASE 2

DISTRIBUTION OF ZONAL AND MERIDIONAL WIND $m\,s^{-1}$

(4°N-18°N)

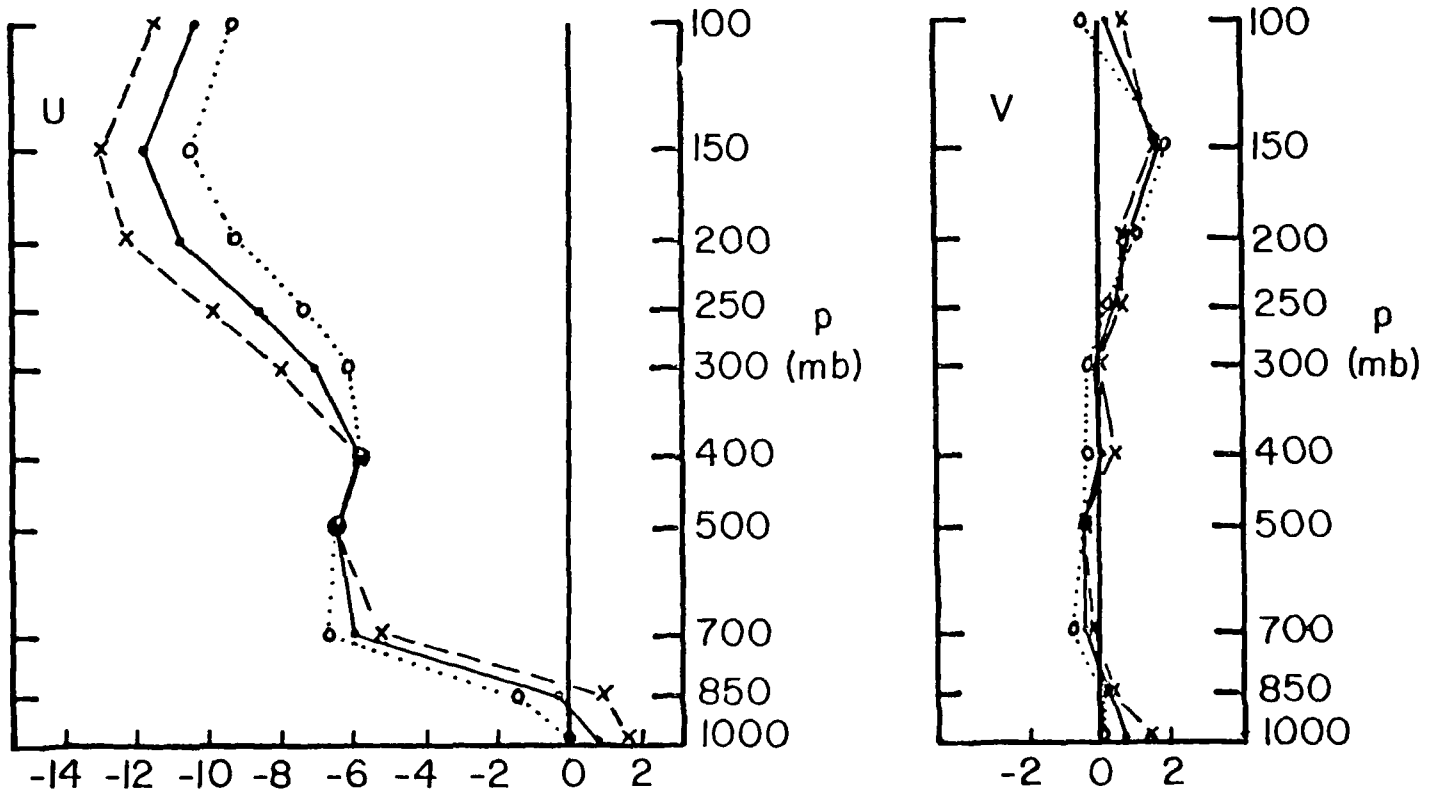

Figure 8

3.2 Horizontal Divergence

Horizontal divergence is examined in the surface-850 mb and 250-200 mb layers (Figure 9). These layers were found to best represent the low level convergence and upper level divergence for the mean state. Two mechanisms account for convergence (divergence): confluence (difluence) in the flow and speed convergence (divergence). Although these mechanisms were not explicitly calculated, it is appropriate to speculate on their importance in certain instances below.

Figure 9 shows an area of maximum low level convergence stretching eastward from the surface col (Figure 4) to western Africa. This convergence is due to both confluence and speed convergence acting in the same sense. In the area of convergence north and east of the Cape Verde Islands, it appears that speed convergence dominates over difluence, while in the divergent area immediately to the east, low level difluence appears to dominate over speed convergence. There is basic agreement over water with the patterns of Tourre et al. (1979); however, over land there are some difference, perhaps due to the different methods of analysis.

Estoque and Douglas (1978) suggest that:

> The pattern of rainfall, cloudiness and water vapor indicate the existence of a vertical circulation whose ascending motion is located about 100 km south of the confluence line and the primary compensating downward motion about 300 km north of the line.

Figure 9. Horizontal divergence ($\nabla_p \cdot \vec{V}$) in $10^{-6}s^{-1}$ for Phase II for surface-850 mb and 250-200 mb layers.

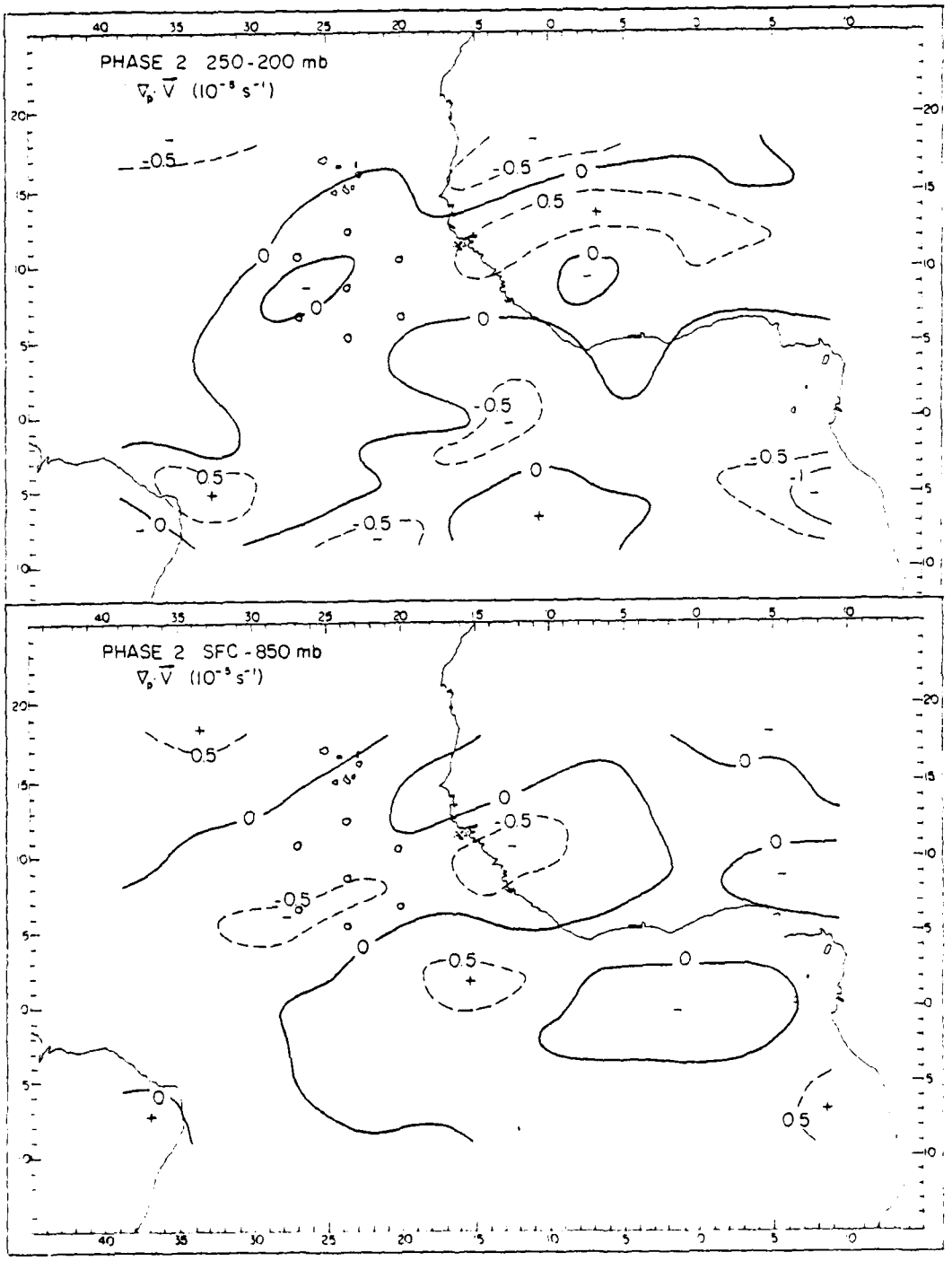
PHASE 2 250-200 mb
$\nabla_p \cdot \overline{V}$ (10^{-5} s^{-1})
PHASE 2 SFC - 850 mb
$\nabla_p \cdot \overline{V}$ (10^{-5} s^{-1})

Figure 9

The low level convergence maximum appears to be about 100 km south of the surface confluence line, while an area of divergence is located approximately 300 km north of the surface confluence line. Sadler (1975) and Ogura and Chen (1979) also have commented on this relationship between the confluence line and cloudiness and/or precipitation.

The horizontal divergence at 250-200 mb (Figure 9) is concommittal with the low level convergence patterns. The divergence over water agrees well with the difluent pattern in the corresponding 200 mb streamline analysis (Figure 4). Generally, in the area west of 20°W, along the 200 mb difluent asymptote (Figure 4), speed convergence dominates to produce convergence. There is good qualitative agreement with Krishnamurti et al. (1978), Pasch et al. (1978) and Tourre et al. (1979) for the upper layer. However, it should be noted that the cited studies were for single levels while this study looks at a layer.

Figure 10 represents the vertical cross-section of $\nabla_p \cdot \vec{V}$ along 13°N. Sadler and Oda (1979) suggest that strong storms moving off the cost encounter an area not conducive to the storms' survival. They note that tropical vorticities during Phase II traveled near 15°N while over land. As they moved off shore the weaker storms turned southward to track along the surface trough near 11°N, while the stronger storms continued westward over water. As seen in Figure 9, the stronger storms that did move westward over water encountered an area where the mean state

Figure 10. Cross-sections of horizontal divergence ($\nabla_p \cdot \vec{V}$) in $10^{-6} s^{-1}$, vertical motion (ω) in 10^{-3}mb s^{-1}, and relative vorticity (ζ) in $10^{-5} s^{-1}$ for Phase II along 13°N.

PHASE 2 $\nabla_p \bar{V}$ (10^{-6} s^{-1})
ALONG 13° N

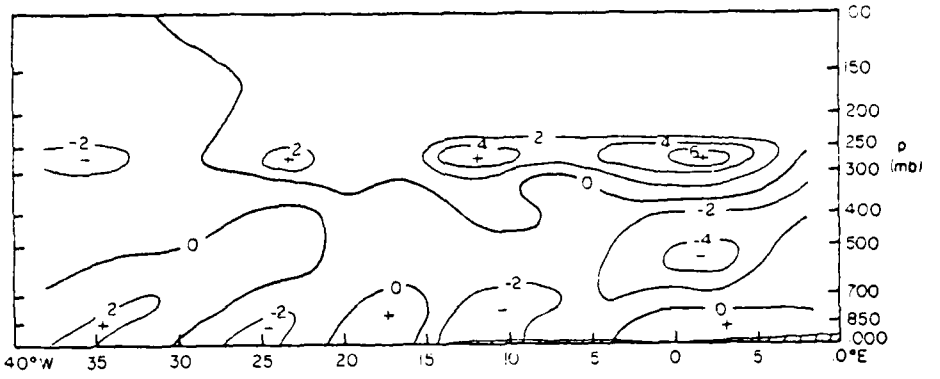

PHASE 2 ω (10^{-3} mb s^{-1})
ALONG 13° N

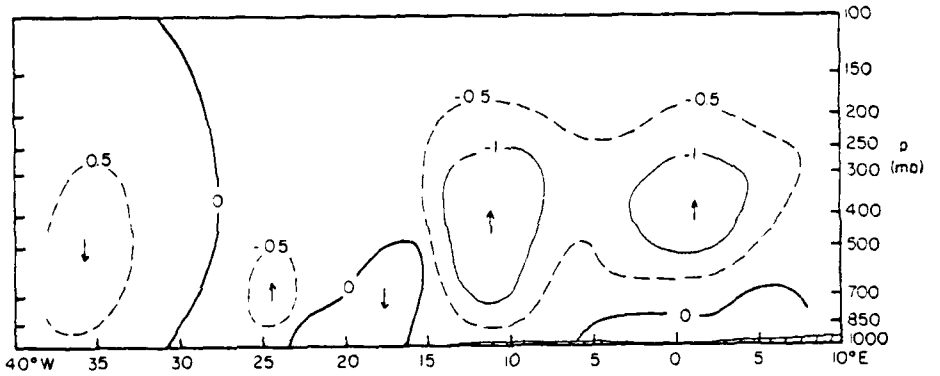

PHASE 2 ζ (10^{-5} s^{-1})
ALONG 13° N

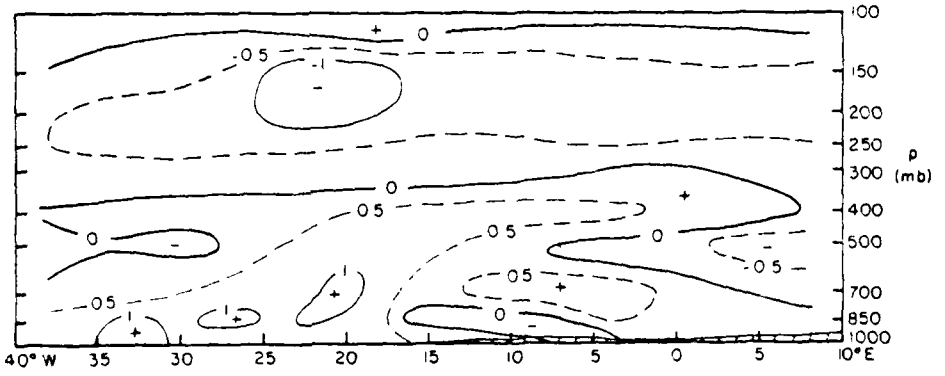

Figure 10

divergence pattern was not conducive to the maintenance of the wave disturbance, namely, low level divergence coupled with upper level convergence. They also point out that storms passing into this area did, indeed, decay. During Phase III, however, this area showed low level convergence with divergence aloft and storms did not decay.

The area of mid-tropospheric convergence over land during Phase II was much different than that during Phase III. By Phase III, weak convergence along the coast was replaced by a strong convergence zone extending to about 400 mb. Low level convergence along the coast, as well as middle level convergence inland, are both coupled with upper level (250 mb) divergence maxima. The secondary low level convergence maximum located near 26°W is related to the speed convergence previously noted. This double maximum, which is weak during Phase II, is prominent in Phase III (Vincent and Scott, 1980).

Figure 11 shows the vertical profile of horizontal divergence over land and water. Low level convergence is associated with the surface confluence zone over water and the 850 mb trough over land. However, above 850 mb, there is convergence over land and weak divergence over water. The level of non-divergence in the mid-troposphere is near 500 mb over water and 350 mb over land. The relative strength of the convergence (divergence) aloft is related to both the depth and intensity of the divergence (convergence) in the lower troposphere and also to the fact that the

Figure 11. As in Figure 8, except for horizontal divergence ($\nabla_p \cdot \vec{V}$) in $10^{-6} s^{-1}$, vertical motion (ω) in 10^{-3} mb s^{-1}, and relative vorticity (ζ) in $10^{-5} s^{-1}$.

PHASE 2 DISTRIBUTION OF $\nabla_p \cdot \vec{V}$ AND ζ ($10^{-6} s^{-1}$) AND ω (10^{-4} mb s^{-1})
(4°N-18°N)

latitude band (38°W-8°E)

over land (14°W-8°E)

over water (38°W-16°W)

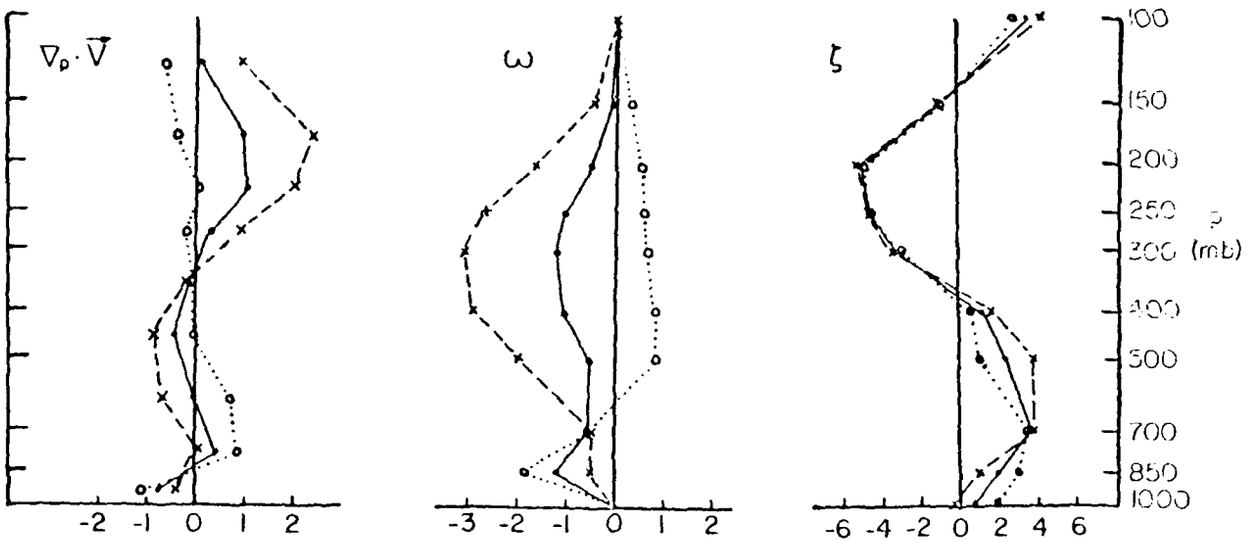

Figure 11

upper level jet is more favorably positioned over land to enhance this result. During Phase III, profiles differed somewhat over water. Low level divergence was much larger in Phase III ($3 \times 10^{-6} s^{-1}$) and the level of non-divergence was near 700 mb. Above 700 mb divergence prevailed throughout the troposphere with only weak convergence in the 150-100 mb layer. This divergence aloft over water during Phase III and convergence aloft during Phase II reinforces the idea that waves moving off the coast during Phase II were moving into an area not conducive to development or maintenance of the wave.

3.3 Vertical Motion

Horizontal maps of vertical motion (ω) are presented in Figure 12 for 700 mb, 500 mb and 300 mb, representative of the lower, middle and upper troposphere, respectively. As expected, areas of upward (downward) motion are highly correlated with areas of low level convergence (divergence) and upper level divergence (convergence). Maximum upward motion over land is in good agreement with the pattern for Phase III (Vincent and Scott, 1980). The maximum along the coast is associated with squall lines developing in this area during the afternoon (Burpee and Dugdale, 1975). The southward shift of the axis of maximum upward motion over water seems to follow the sea surface temperature maximum.

The main difference in the vertical motion patterns between Phase II and Phase III occur over water.

Figure 12. Vertical motion (ω) in 10^{-3} mb s^{-1} for Phase II at 700 mb, 500 mb, and 200 mb.

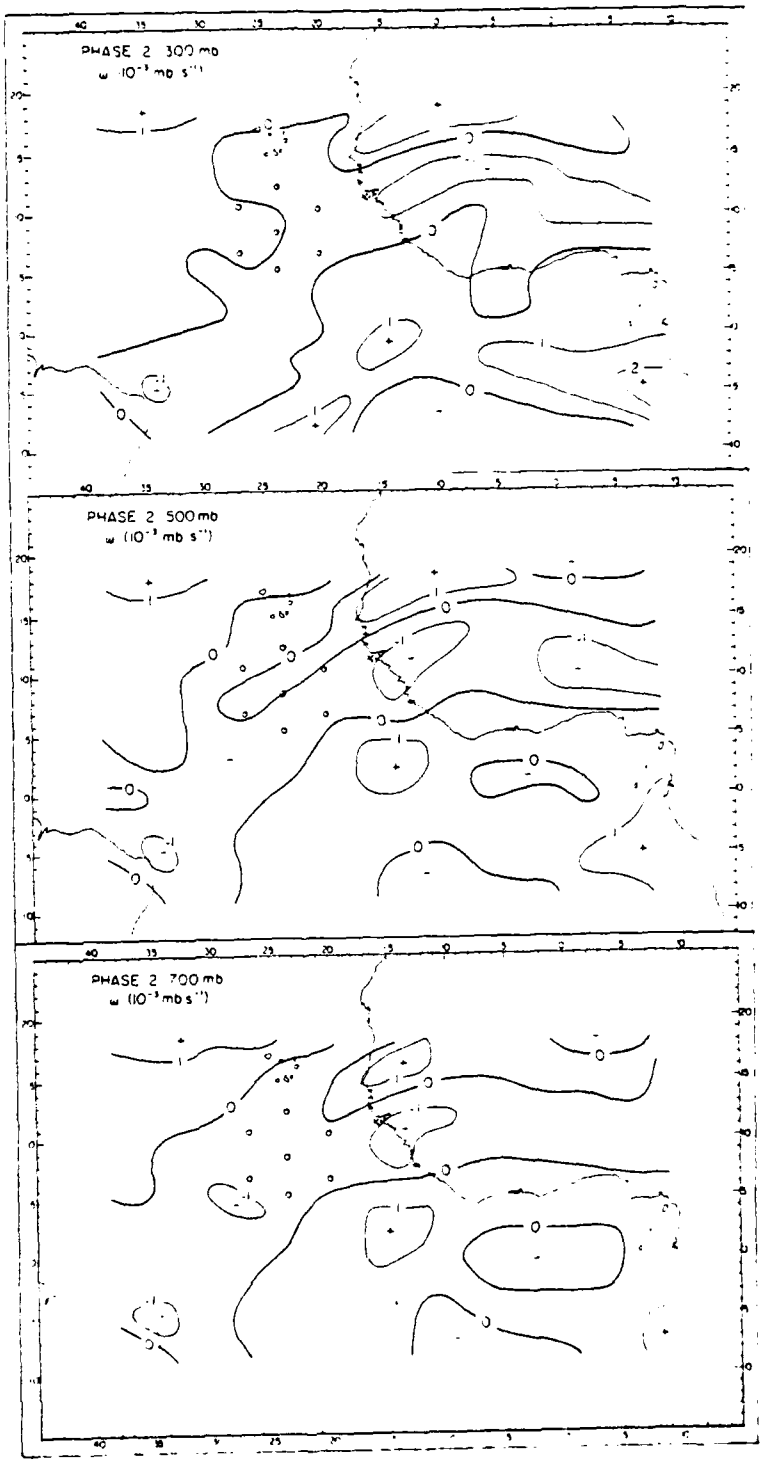

Figure 12

During Phase II the vertical motion over much of the water subregion was downward. This is evident from the divergence patterns in Figure 9. Downward motion occurred during Phase III but, in general, it did not reach the surface. During Phase III upward motion extended along 12°N across Africa and out over the water. As noted above, there was a distinct southward shift of the upward motion zone over water during Phase II, while west of of 30°W and north of 5°N there is downward motion. Thus, storms moving westward along 15°N (the average storm track over land during Phase II) and along 13°N (the average storm track over land during Phase III) encountered different environments as they moved off shore.

Figure 13 shows the vertical motion along 24°W and 4°W. The double maximum of upward motion along 24°W at 15°N and 5°N are similar to the pattern for Phase III (Vincent and Scott, 1980); however, values were much larger during Phase III. The northern maximum is associated with the storm track and is a reflection of the transient waves in the mean state. The southern maximum is associated with the confluence zone (Figure 4) and more a manifestation of the mean state than transient wave influences. Over land at 4°W upward motion reflects the higher level of non-divergence and the deep layer of convergence (Figure 11).

The vertical cross-section of ω along 13°N is presented in Figure 10. Most noteworthy is the area of downward

Figure 13. As in Figure 6, except for vertical motion in 10^{-3} mb s^{-1}.

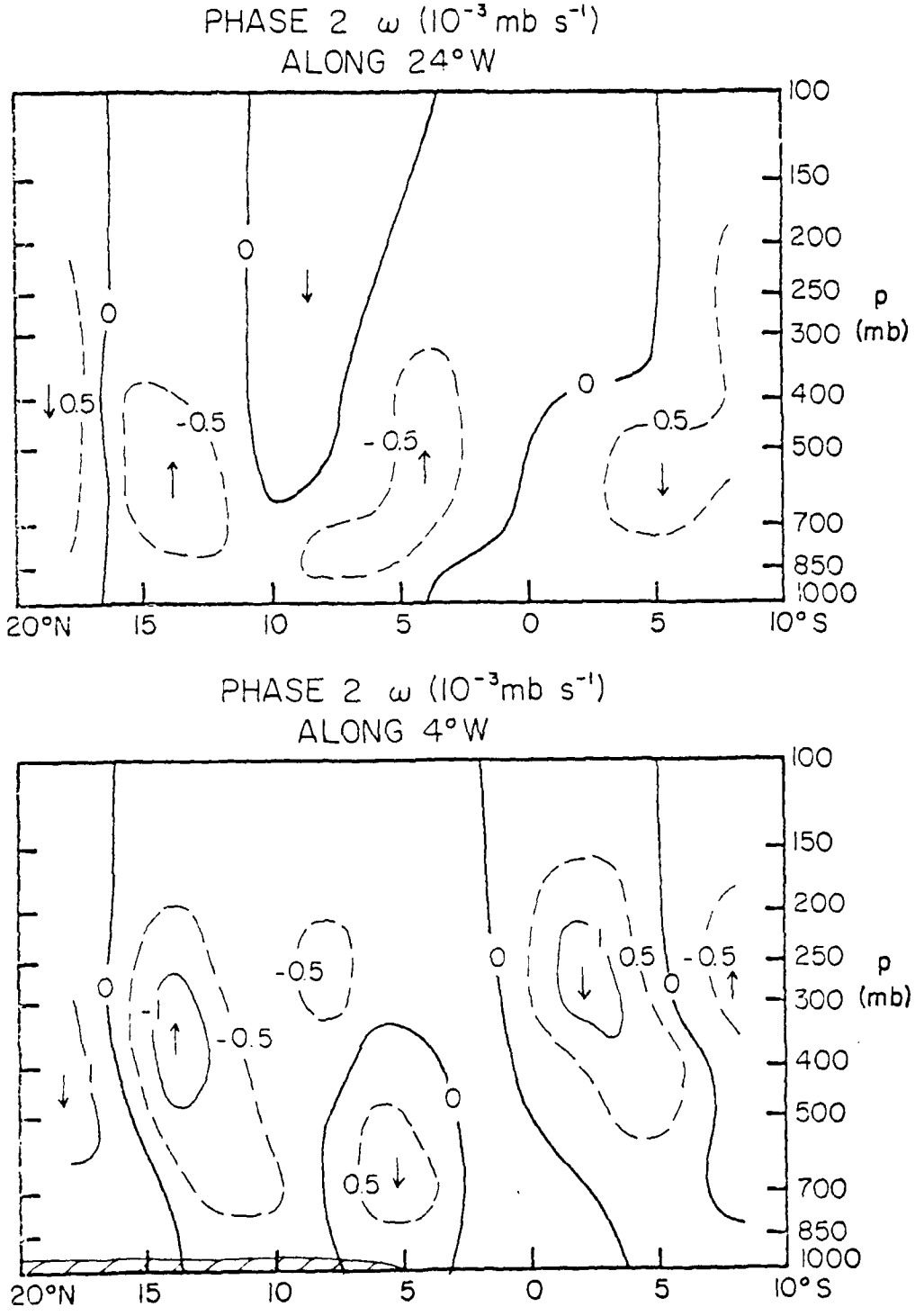
PHASE 2 ω (10^{-3} mb s^{-1})
ALONG 24°W
100
150
200
250
300
400
500
700
850
1000
p (mb)
0
0
0
0
0.5
-0.5
-0.5
0.5
20°N
15
10
5
0
5
10°S
PHASE 2 ω (10^{-3}mb s^{-1})
ALONG 4°W
100
150
200
250
300
400
500
700
850
1000
p (mb)
0
0
-0.5
-0.5
0
0.5
0
0.5
-0.5
0
20°N
15
10
5
0
5
10°S

Figure 13

motion west of 30°W. As noted earlier, westward propagating waves entering this area along 13°N encounter unfavorable conditions for enhancement or survival. This area did not contain downward motion during Phase III.

Figure 11 represents the vertical profile of ω averaged over land and water. The pattern reflects the divergence profile with maximum upward motion near 350 mb, the level of non-divergence. Note that there is, on the average, downward motion over water above 700 mb.

3.4 Relative Vorticity

Horizontal maps of relative vorticity at 850 mb, 700 mb and 200 mb are shown in Figure 14. Two mechanisms contribute to vorticity: horizontal wind shear and curvature of the flow, where cyclonic circulation and wind shear are associated with positive vorticity. At 850 mb anticyclonic circulation associated with cross equatorial flow dominates over cyclonic wind shear resulting in negative vorticity south of 8°N. Positive vorticity to the north is related to cyclonic flow around the heat low over the Sahara Desert which dominates the anticyclonic wind shear. This pattern is similar to that of Phase III (Vincent and Scott, 1980). However, the negative area over the African coast near 13°N does not appear in the Phase III mean state. Both the location of the positive maximum and the location of the negative maximum are in excellent quantitative and qualitative agreement with Tourre et al. (1979). This negative maximum

Figure 14. Relative vorticity (ζ) in $10^{-5}s^{-1}$ for Phase II at 850 mb, 700 mb and 200 mb.

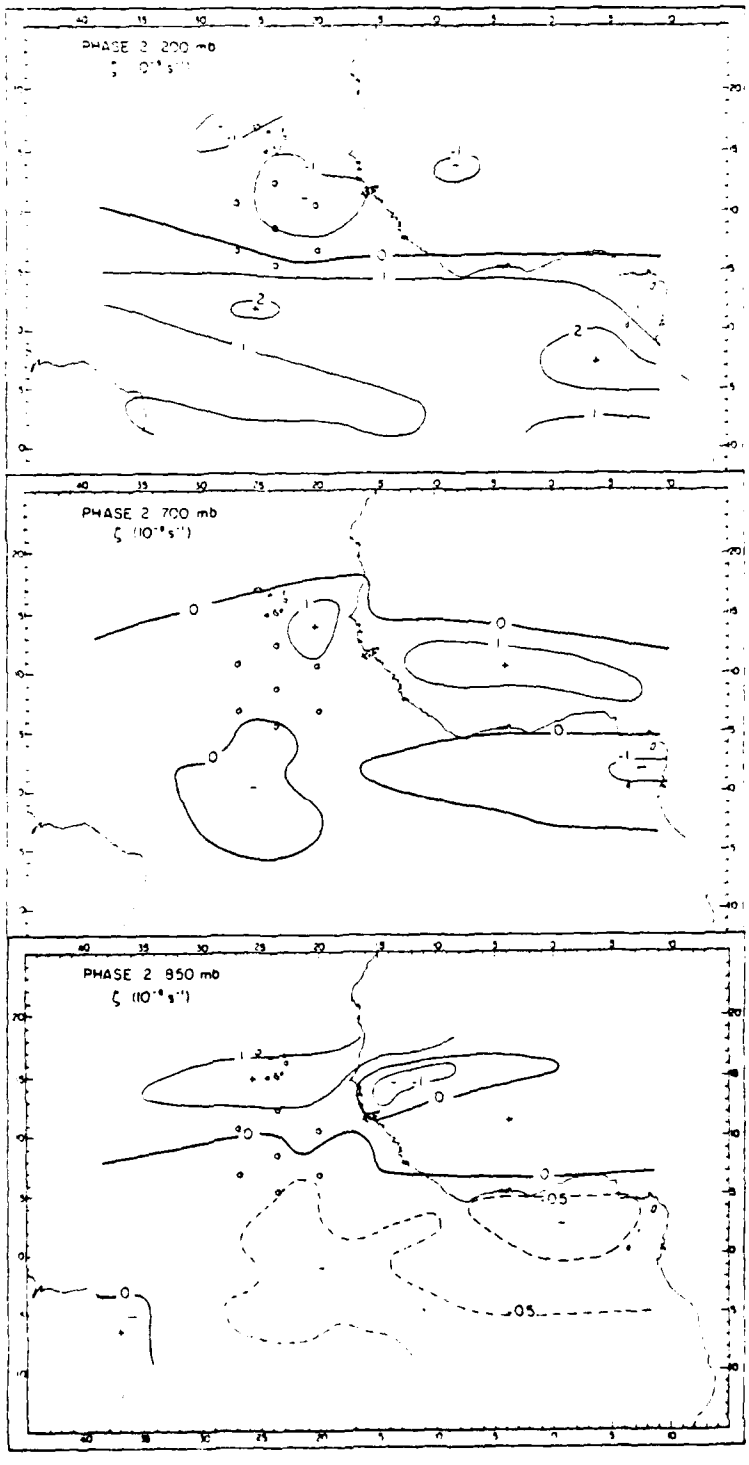

Figure 14

seems to be associated with the anticyclonic circulation near the coast and is not too dependent on wind shear. At 700 mb and 200 mb, the patterns are closely related to the jet activity with the zero lines being in very good agreement with the axes of the respective jets (Figure 4). In both cases anticyclonic flow and anticyclonic wind shear occur to the north of the jet and cyclonic flow and cyclonic wind shear to the south. At 850 mb and 700 mg, the negative vorticity along the southern coast of the African bridge and the Bay of Guinea is associated with anticyclonic wind shear dominating over cyclonic flow.

Figure 15 depicts vertical cross-sections along 24°W and 4°W. The positive vorticity pattern associated with the mid-tropospheric jet is at a lower height over water (Figure 6). Note that the negative value south of 5°N associated with the cross-equatorial flow only extends up to about 700 mb, indicating that the low level flow pattern is relatively shallow.

Figure 10 shows the vertical cross-sectional analysis along 13°N. As expected, positive vorticity dominates in the lower and middle troposphere with negative vorticity above. While this pattern is in good agreement with the Phase III results of Vincent and Scott (1980), magnitudes in the vicinity of the maxima tend to be smaller in Phase II.

Figure 15. As in Figure 6, except for relative vorticity in $10^{-5}s^{-1}$.

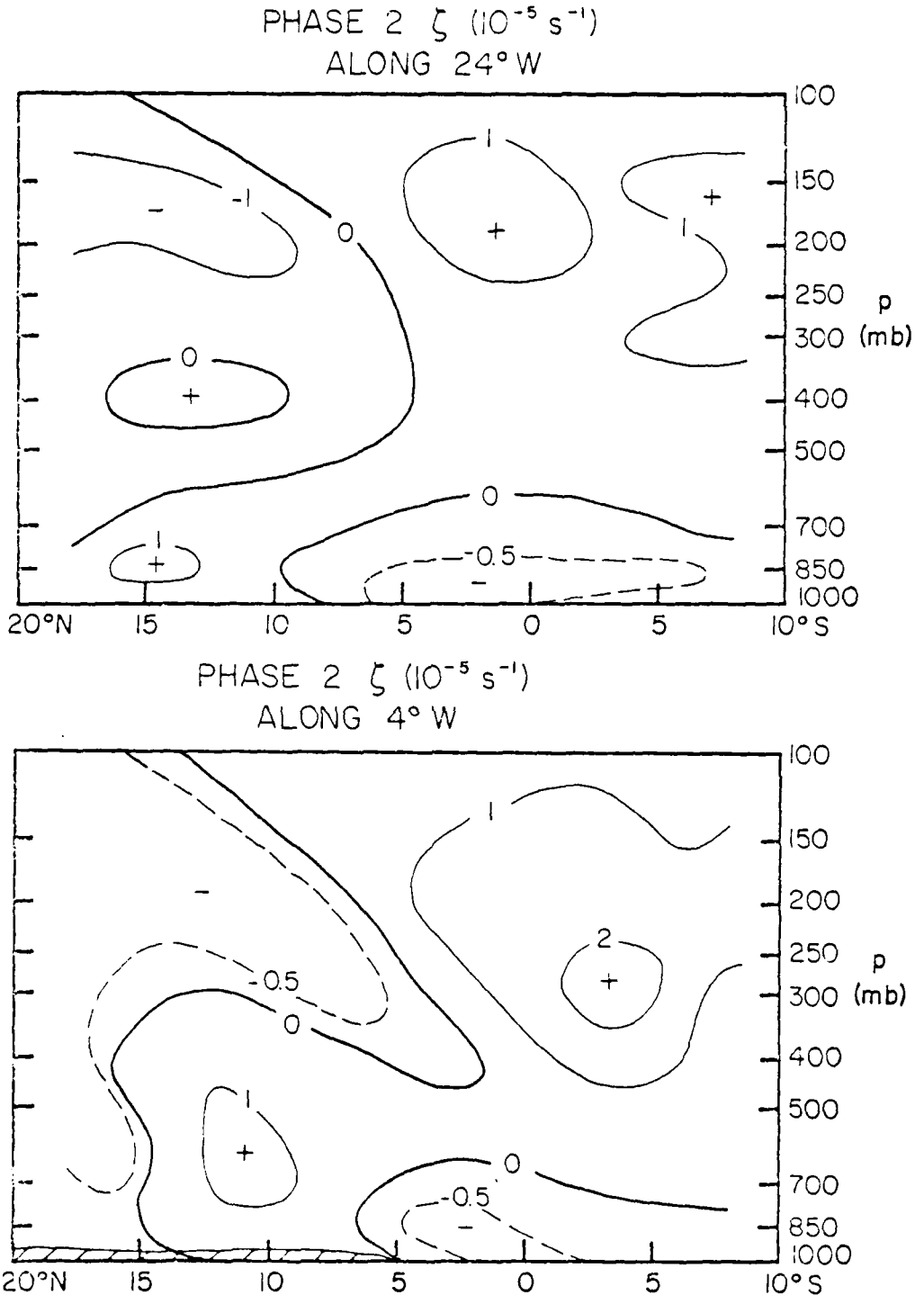
PHASE 2 ζ (10⁻⁵ s⁻¹)
ALONG 24° W
100
150
200
250
300
400
500
700
850
1000
p (mb)
20°N
15
10
5
0
5
10° S
PHASE 2 ζ (10⁻⁵ s⁻¹)
ALONG 4° W
100
150
200
250
300
400
500
700
850
1000
p (mb)
20°N
15
10
5
0
5
10° S

Figure 15

Figure 11 depicts the vertical profiles of relative vorticity over land and water. The large positive values over water at low levels reflect the location of the positive maximum over water. Above 700 mb, the patterns appear similar over land and water. At 500 mb over water the flow shows slight cyclonic curvature, but the wind shear is anticyclonic. Over land, cyclonic wind shear and cyclonic curvature dominate to produce positive vorticity. The net result is that positive vorticity over land is stronger than over water. This profile is similar to that of Phase III (Vincent and Scott, 1980); however, the magnitudes during Phase III range from $5 \times 10^{-6} s^{-1}$ at 850 mb to $-9 \times 10^{-6} s^{-1}$ near 200 mb.

Gray (1978) and McBride (1979) suggest that an important measure of the intensification of cloud clusters into wave disturbances is the vertical vorticity shear, i.e., $\zeta_{900} - \zeta_{200}$. Gray (1978) composited both developing and non-developing cloud clusters in the western Pacific. He found that within a 4° radius from the center of the developing composite cluster, the mean vertical vorticity shear was $3.1 \times 10^{-5} s^{-1}$. It is interesting to compare this value with that obtained using mean state data in the present study (Figure 16). The maximum value of $\zeta_{850} - \zeta_{200}$ is $2.5 \times 10^{-5} s^{-1}$ located south and east of the Cape Verde Islands. The average value for all points within a 4° radius of this maximum is $2.1 \times 10^{-5} s^{-1}$. Also, as noted

Figure 16. Vertical shear of relative vorticity ($\zeta_{850}-\zeta_{200}$) in $10^{-5}s^{-1}$.

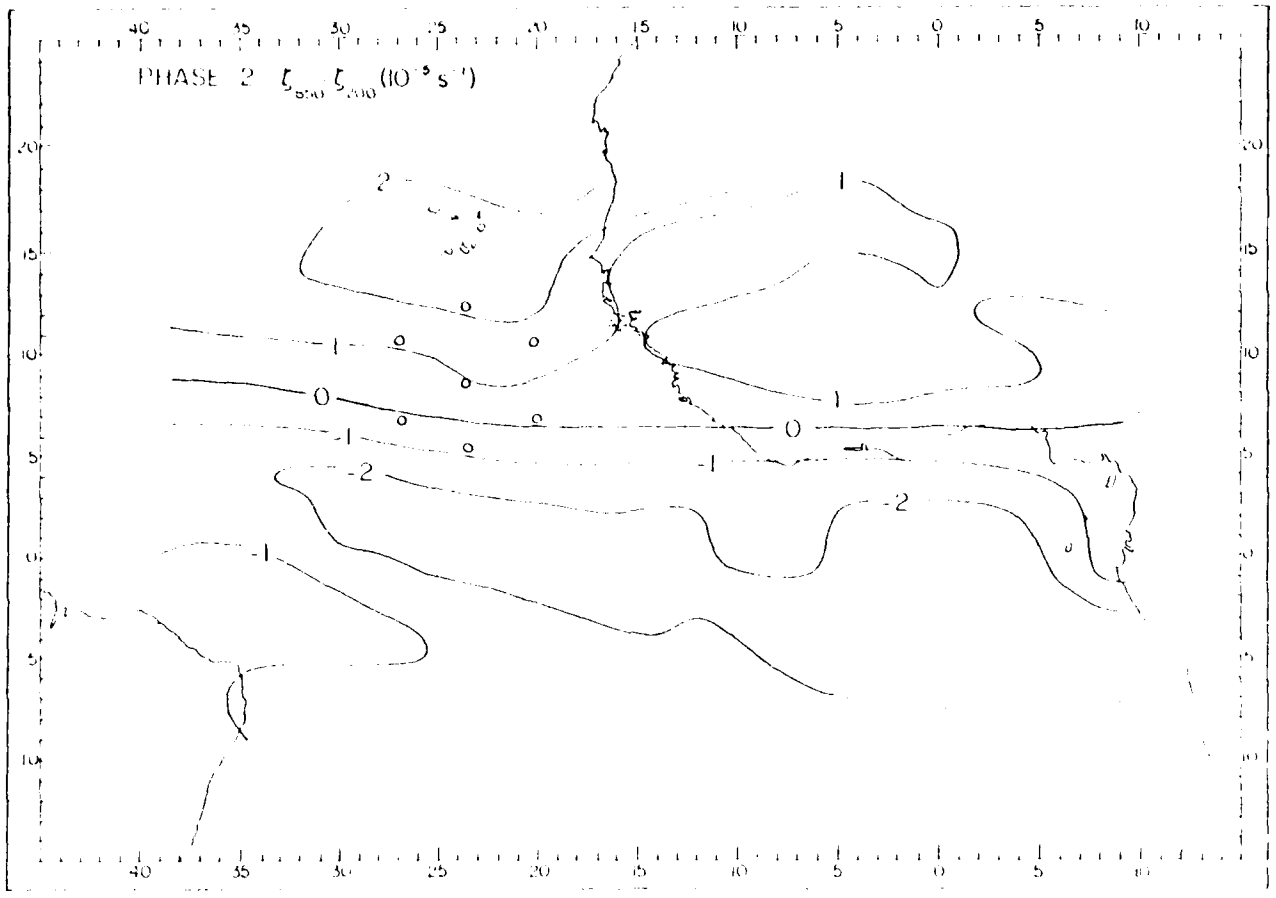

Figure 16

earlier, there is downward motion in this area, and according to Sadler and Oda (1979) many of the waves traversing this region during Phase II decayed.

Kuo (1949) notes that a necessary condition for barotropic instability is $\partial(f-\partial u/\partial y)/\partial y = 0$. Several investigators (e.g., Burpee and Dugdale, 1975; Reed et al., 1978; Vincent and Scott, 1980) have shown that, both over land and water, this condition existed during Phase III in the region of the mid-tropospheric jet. Figure 17 shows that this condition also existed in Phase II. Though the condition (zero line) exists north and south of the mid-tropospheric jet (Figure 4) the southern, or cyclonic, side is the preferred location of wave development for this instability region.

3.5 Vorticity Budget

Figure 18 shows vertical profiles of the five components of the vorticity equation, (equation 7), given earlier. Positive values of these quantities correspond to sources of vorticity, while negative values represent sinks. For HADV and VADV, a source region requires transport of vorticity down the gradient of vorticity, while a sink requires counter-gradient transport.

Figure 18 shows that HADV acts as an important source of vorticity over water in the 800-350 mb layer and as a sink elsewhere. Over land, this term acts as a sink of vorticity at all levels. In the lowest layer, over water

Figure 17. Cross-section of meridional gradient of absolute vorticity averaged for water and land subregions in 10^{-13} s^{-1} m^{-1}.

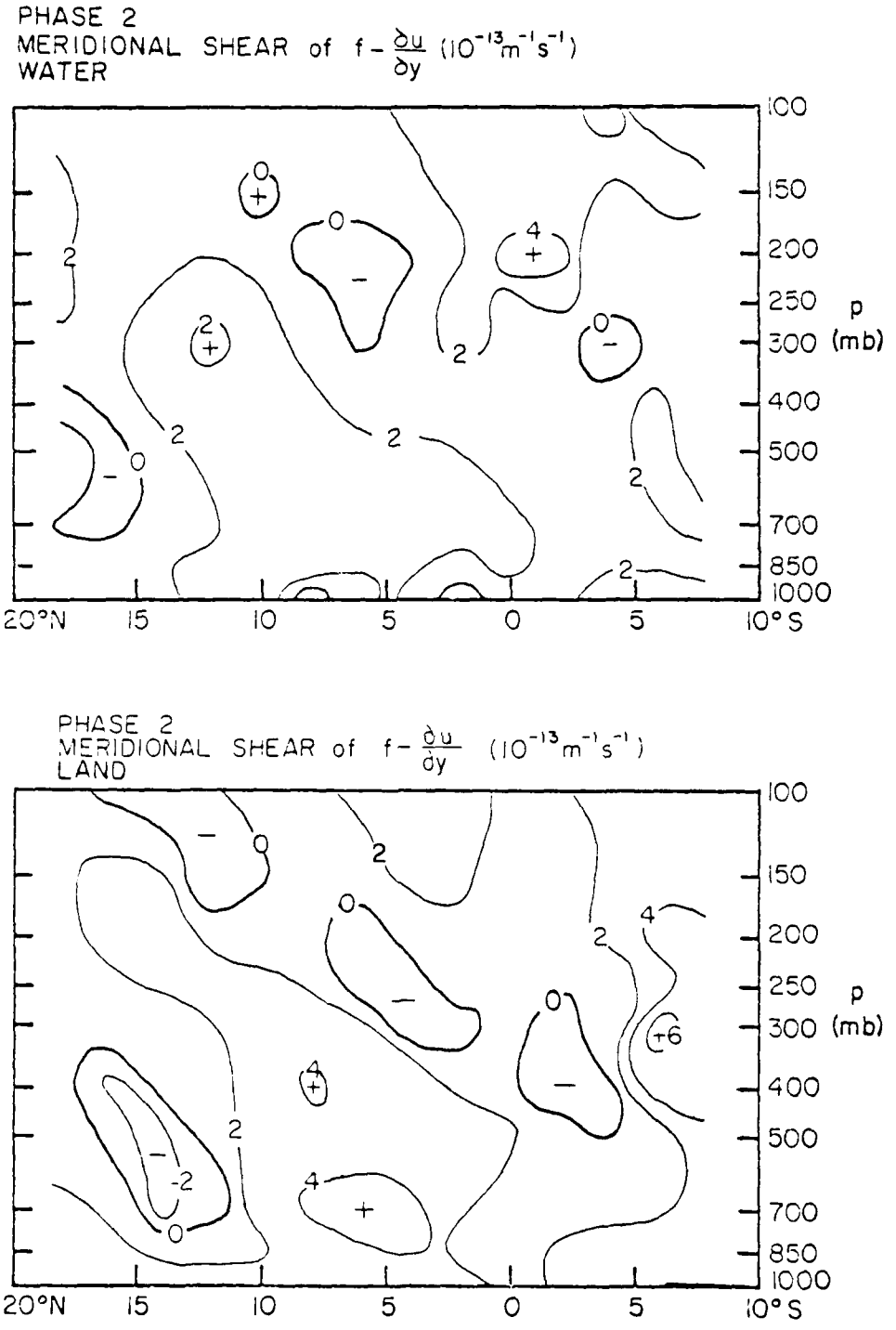
PHASE 2
MERIDIONAL SHEAR of $f-\frac{\partial u}{\partial y}$ $(10^{-13}m^{-1}s^{-1})$
WATER
100
150
200
250
300
400
500
700
850
1000
p
(mb)
20°N
15
10
5
0
5
10°S
PHASE 2
MERIDIONAL SHEAR of $f-\frac{\partial u}{\partial y}$ $(10^{-13}m^{-1}s^{-1})$
LAND
100
150
200
250
300
400
500
700
850
1000
p
(mb)
20°N
15
10
5
0
5
10°S

Figure 17

Figure 18. As in Figure 6, except for vorticity budget terms in $10^{-11}s^{-1}$, see text for details.

PHASE 2 DISTRIBUTION OF ζ BUDGET TERMS (4°N-18°N)
(10^{-11} s^{-2})

latitude band (38°W-8°E)

over land (14°W-8°E)

over water (38°W-16°W)

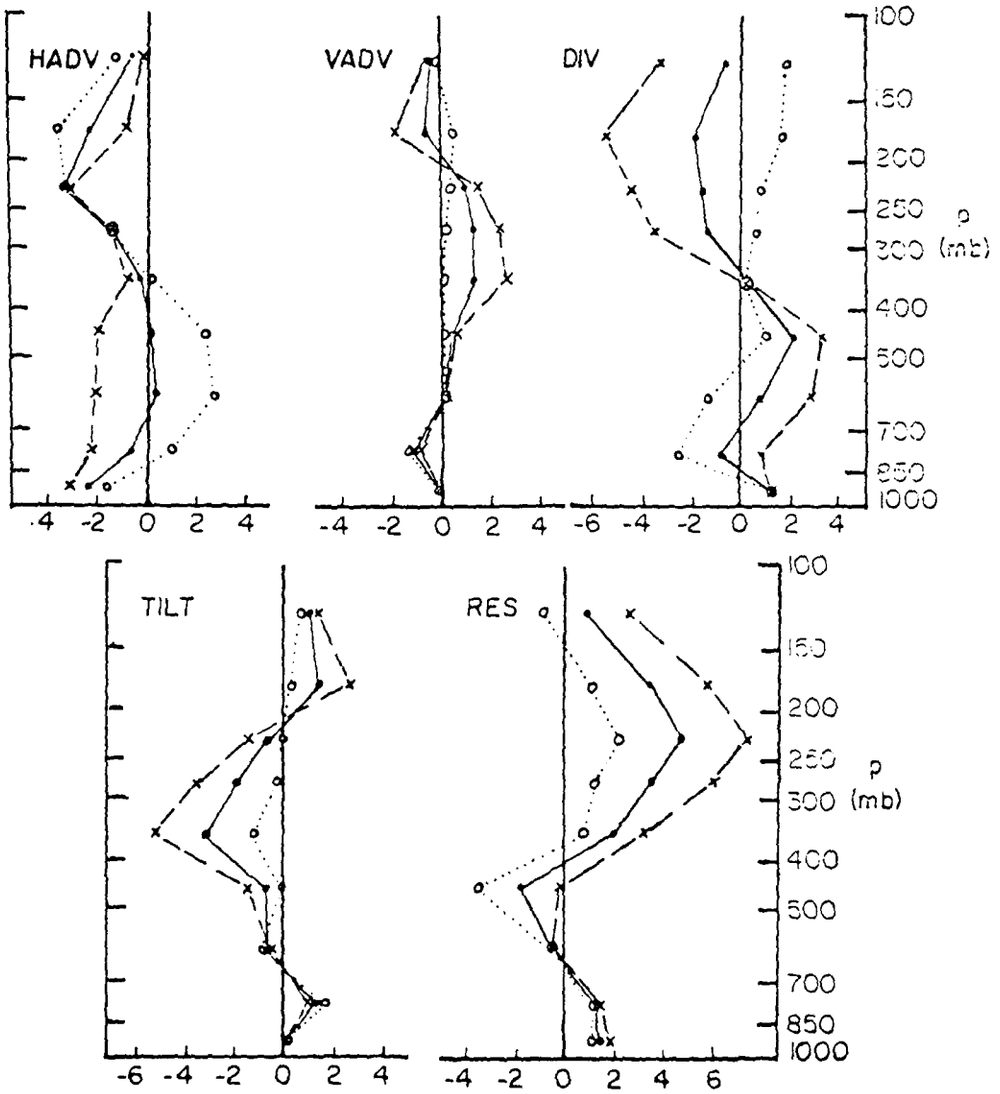

Figure 18

northerly flow north of the vorticity maximum and southerly flow south of the maximum account for transport of vorticity-poor air into the area. Over land, southerly flow advects more anticyclonic (less cyclonic) air into the area (Figures 4 and 14). Between 800 and 350 mb, easterly flow dominates and the location of the vorticity maximum along the coast accounts for transport of cyclonic vorticity from land to water and the resultant source (sink) over water (land). Above 350 mb there is a counter-gradient transport of vorticity by the zonal wind component both over land and water. However, over water the zonal wind isn't as dominant as over land.

The vertical advection term, VADV, indicates that vorticity-rich air is being transported upwards from the lower troposphere to the middle and upper troposphere. Above 400 mb, the profile over land shows higher positive values than over water due to more cyclonic (less anticyclonic) vorticity and a greater intensity of upward motion over land (Figure 11).

Since the absolute vorticity is positive throughout the land and water subregions, the sign of the DIV term is influenced by the sign of the horizontal divergence. Thus, convergence represents a vorticity source, and divergence a vorticity sink. Over water, the mid-tropospheric source is replaced by a weak sink at upper levels, related to the convergence aloft and associated downward motion in the

area. Basic differences of the DIV term between Phase II and Phase III are related to differences in convergence and divergence patterns discussed previously (Figure 11). To a large extent, the DIV term balances the HADV term in the lower troposphere.

In the 600-200 mb layer, the TILT term is a major vorticity site over land. Over water it also acts as a sink but is smaller in magnitude. A physical interpretation of this term is difficult; however, an examination of its two components, $\partial\omega\partial u/\partial y\partial p$ and $-\partial\omega\partial y/\partial x\partial p$, was conducted (Figures 4, 10, 11 and 12, as well as others not shown). Both components are found to be important and contribute to the sign of TILT. A careful examination reveals that the first term is negative over land but positive over water. The second term, with the sign, is negative over both land and water. The net effect is a larger negative value over land than water.

As noted in Chapter 2, the RES term is influenced by three basic factors: time departure terms due to transient wave grid-scale phenomena, frictional effects of the mean state and errors in the other calculated terms in the equation. To act as a true balance term in this equation, RES must also include subgrid/grid scale interactions, which are not present in the time mean state vorticity equation. Since none of these influences can be directly estimated, a physical interpretation of RES is difficult. Nevertheless, since the profiles over land and water parallel each other,

it is reasonable to speculate on which of the mechanisms listed above might be dominant at various levels. It can be argued that the effect of the friction term, represented in the RES term as $\frac{\partial F_y}{\partial x} - \frac{\partial F_x}{\partial y}$, has little effect above the planetary boundary layer, except possibly near the level of the upper tropospheric jet. Therefore, in the region above 400 mb, where large positive values of RES occur, if errors are negligible, two effects are responsible for the computed source of vorticity: time departures related to grid-scale phenomena and subgrid-to-grid-scale processes. Results of the present study are at least qualitatively similar to other studies where the RES term has been estimated (e.g., Daggupaty and Sikka, 1977, for Bay of Bengal monsoon depressions over northern India; Stevens, 1979, for large sacle waves during Phase III; Vincent and Waterman, 1979, for intensification of hurricane Carmen in the Caribbean). In all three cases the authors suggest that widespread cumulus convection is partially responsible for the upward transport of subgrid-scale cyclonic vorticity which ultimately becomes large scale vorticity in the middle and upper troposphere. It has been suggested by Holton and Colton (1972) and Chu (1976) that this type of mechanism is present in active tropical systems. Deep convection did occur during Phase II, although it was not as intense as in Phase III; thus, it appears plausible that this effect contributed somewhat to increases in vorticity above 400 mb. It is noteworthy that, although the magnitude of the RES

term during Phase III is similar over water, over land the value during Phase II is considerably larger. Thus, a sub-grid to grid scale transfer of vorticity does not offer a complete explanation. Therefore, it may suggest that large-scale transient waves are a more important source of vorticity in the upper troposphere during Phase II than during Phase III.

Daily maps of streamlines and wind speeds at 250 mb (Sadler and Oda, 1979) were inspected in an effort to determine to what extent the upper tropospheric jet varied. It was found that there was both latitudinal and speed variation of the maximum wind. This suggests that not only were large-scale eddies present, but that the jet seemed to pulsate in the zonal plane. The combination of these two effects could account for part of the large positive value in the upper troposphere.

Below 700 mb, this term also acts as a source of vorticity. Assuming that the magnitude of friction is proportional to the magnitude of the wind speed, but acts in the opposite direction. This term may be examined through an analysis of the wind field (Figure 4) where

$$\frac{\partial F_y}{\partial x} \propto -\frac{\partial v}{\partial x} \qquad \text{and} \qquad \frac{\partial F_x}{\partial y} \propto -\frac{\partial u}{\partial y} \tag{8}$$

Equation (8) implies that over land the term $\partial F_y/\partial x$ is nearly zero, whereas $-\partial F_x/\partial y$ is positive. Over water $\partial F_y/\partial x$ is positive, while $-\partial F_x/\partial y$ is negative but small.

Hence, friction acts as a source both over land and water.

Figure 11 reveals that in the 700-200 mb layer deep cumulus convection would act as a source of vorticity, transporting more cyclonic (less anticyclonic) vorticity aloft. Thus, the sink region over water in the 600-400 mb layer must be the result of other mechanisms. If we assume that the errors in the other terms are negligible and that the frictional term is negligible above the planetary boundary layer, we are left with time deviations due to synoptic-scale wave disturbances as the probable cause of this sink region. Although wave disturbances during Phase II had their maximum amplitude near 700 mb, some on occasion penetrated to near the 500 mb level.

CHAPTER 4

CONCLUSIONS

This study investigated the kinematic parameters of the large-scale (A-scale) tropical mean state flow over the eastern Atlantic and western Africa during Phase II of GATE. Subjective analyses of wind direction and speed, horizontal wind components, and temporal standard deviation of the horizontal wind components were performed for all mandatory pressure levels from the surface to 100 mb, using the FVDS for GATE phase means. Horizontal divergence, vertical (p) velocity and relative and absolute vorticity, as well as terms in the vorticity equation, were also derived and subjectively analyzed.

Results were compared to the Phase III results of Vincent (1980) and Vincent and Scott (1980), as well as to those of other investigators working with GATE data in the same area. Results were also presented separately for the land and water subregions.

It has been shown that wind patterns in the lower troposphere during Phase II were in good agreement with long-term means for the GATE region. Low level westerlies associated with the monsoon circulation and the Sahara heat low gave way to easterlies above 800 mb with the mid-tropospheric jet maximum located near 650 mb at 16°N over water and 14°N

over land. This position is 1° to 2° north of the position during Phase III. The barotropic instability criterion of Kuo (1949) was met both over land and water in association with the mid-tropospheric jet. Along the average wave disturbance track for Phase II (13°N), low level convergence over water was rapidly replaced by divergence west of 35°W. This represented one of the primary differences between Phase II and Phase III. Along the Phase III mean disturbance track (11°N), low level convergence existed throughout the area of analysis.

An upper level jet, located at about 6°N and 200 mb, sloped poleward and upward and was the main feature in the upper troposphere. The position of the upper level jet was 2° north of its Phase III position but the two strengths were comparable. Upper level divergence over land gave way to convergence over water west of 30°W, particularly along the average disturbance track. This upper level convergence was replaced by upper level divergence during Phase III. Since low level divergence, which occurred during Phase II over water, was replaced by low level convergence during Phase III, the mean state conditions in Phase III were more favorable for maintenance of the large-scale waves that propagated out over the eastern Atlantic.

Since vertical velocity patterns reflect the divergence patterns, there was good agreement between the two phases over land, but not over water. It was noticed that the

magnitudes during Phase III were larger than those during Phase II.

Low level vorticity patterns for both phases revealed cyclonic vorticity north of the surface confluence zone over land and water. Similarly, negative vorticity prevailed throughout the upper troposphere during both phases. Vertical shear of absolute vorticity between 850 mb and 200 mb was positive north of 8°N. Although the shear was greatest over water, it was still less than Gray's (1978) critical value for intensification of cloud cluster scale disturbances.

The vorticity budget revealed that all terms in (7) made significant contributions. The residual term, RES, was found to be large in the upper troposphere and near the surface. The values of the residual in the upper troposphere during Phase II were found to be larger than those during Phase III. This source of vorticity appears to be due primarily to the temporal variation of synoptic scale transient features.

It should be remembered that the results presented in this study represent time-mean quantities for a 21 day period during the mid-summer of 1974 in the Northern Hemisphere and, therefore, should not be over-generalized. Since the prior climatology of this region has been confined to the surface over the eastern Atlantic, the present results represent a valuable contribution to the picture for this region.

At present, additional research involving heat, moisture and energy budget studies are being conducted for Phases II and III. In the future, it is planned to extend our phase mean analyses to include Phase I. Comparison of these and other studies, both on a phase-to-phase basis and with the general climatology, should lead to a better understanding of the tropical atmosphere, the role it plays in the general circulation and the role that scale interaction plays in the life cycle of tropical weather systems.

REFERENCES

REFERENCES

Aspliden, C.I., 1974: The low level wind fields and associated perturbations over tropical Africa during northern summer. Preprint from Internat'l Tropical Meteorology Meeting, Nairobi, Kenya, Part 1, 218-233.

Aspliden, C.I., Y. Tourre and J.B. Sabine, 1976: Some climatological aspects of west African disturbance lines during GATE. Mon. Wea. Rev., 104, 1029, 1035.

Burpee, R.W., 1972: The origin and structure of easterly waves in the lower troposphere of north Africa. J. Atmos. Sci., 29, 77-90.

Burpee, R.W., and G. Dugdale, 1975: A summary of weather systems affecting western Africa and the eastern Atlantic during GATE. GATE Report No. 16, ICSU,WMO, Geneva, Switzerland, 2.1-2.42.

Carlson, T.N., 1969: Some remarks on African disturbances and their progress over the tropical Atlantic. Mon. Wea. Rev., 97, 256-276.

Carlson, T.N. and S.G. Benjamin, 1980: Radiation heating rates for Sahara dust. J. Atmos. Sci., 37, 193-213.

Chu, J., 1976: Vorticity in maritime cumulus clouds and its effect on the large-scale budget of vorticity in the tropics. Tropical Meteorology Paper No. 17, Department of Atmospheric Sciences, University of California, Los Angeles, 123 pp.

Depradine, C., R. Pasch and T. Krishnamurti, 1978: An atlas of the motion field over the GATE area, Part III (900 mb). Report No. 78-3, Department of Meteorology, Florida State University, Tallahassee, 133 pp.

Daggupathy, S.M. and D. Sikka, 1977: On the vorticity budget and vertical velocity distribution associated with the life cycle of a monsoon depression. J. Atmos. Sci., 34, 773-792.

Estoque, M.A. and M. Douglas, 1978: Structure of the intertropical convergence zone over the GATE area. Tellus, 30, 55-61.

Frank, N., 1969: The inverted v cloud pattern-an easterly wave? Mon. Wea. Rev., 97, 130-140.

Frank, N., 1975: Atlantic tropical systems of 1974. Mon. Wea. Rev., 103, 294-300.

Gray, W.M., 1978: Hurricanes/their formation, structure and likely role in the tropical circulation. Paper prepared for R. Met. Soc. conference on meterology over the tropical ocean. London, 117 pp.

Gray, T., J. Irwin, A. Kruger and M. Varnadore, 1976: Average Circulation in the Troposphere over the Tropics. Department of Commerce.

Holton, J. and D. Colton, 1972: A diagnostic study of the vorticity balance at 200 mb in the tropics during the northern summer. J. Atmos Sci., 29, 1124-1128.

Krishnamurti, T.N., P. Pasch and C. Depradine, 1978: An atlas of the motion fields over the GATE area, Part I (200 mb). Report No. 78-2, Department of Meteorology, Florida State University, Talahassee, Florida, 133 pp.

Kuettner, J.P., 1974: General description and central program of GATE. Bull. Amer. Meteor. Soc., 55, 711-719.

Kuo, H., 1949: Dynamical instability of 2-dimensional non-divergent flow in a barotropic atmosphere. J. Meteor. 6, 105-122.

McBride, J.L., 1979: Observational analysis of tropical cyclone formation. Paper No. 308, Colorado State University, Department of Atmospheric Sciences, Fort Collins, Colorado.

Newell, R.E., J.W. Kidson, D.G. Vincent and G.J. Boer, 1972: The General Circulation of the Tropical Atmosphere and Interactions with Extratropical Latitudes Volume 1. MIT Press, Cambridge, Mass., 237 pp.

Nicholson, S.E., 1975: Variations of the intertropical convergence zone during phases 1, 2, and 3 of the GATE experiemnt. GATE Report No. 14, ICSU, WMO, Geneva, Switzerland, 169-175.

O'Brien, J.J., 1970: Alternative solutions to the classical vertical velocity problem. J. Appl. Meteor., 9, 197-203.

Ogura, Y. and Y.L. Chen, 1979: Relationship between large-scale forcing and precipitation observed in GATE. GATE seminar on the impact of GATE in large-scale numerical modeling of the atmosphere and ocean. Woods Hole, Ma., National Academy of Science, Washington, D.C., 10 pp.

Pasch, R., T. Krishnamurti and C. Depradine, 1978: An atlas of the motion field over the GATE area, part II (250 mb). Report No. 78-3, Department of Meteorology, Florida State University, Talahassee, Florida, 133 pp.

Reed, R.J., D. Norquist and E.E. Recker, 1977: The structure and properties of African wave disturbances as observed during phase III of GATE. Mon. Wea. Rev., 105, 317,333.

Sadler, J.C., 1975: The monsoon circulation and cloudiness over the Gate area. Mon. Wea. Rev., 103, 369-387.

Sadler, J.C. and L. Oda, 1979: The synoptic la. scale circulation during the second phase of GATE, 17 July-19 August 1974. UHMET 79-14, Dept. of Meteorology, University of Hawaii, Honolulu, Hawaii, 36 pp.

Scott, G., 1980: Kinematic analysis of the mean state of the tropical atmosphere over the eastern Atlantic ocean and western Africa during phase 3 of GATE. M.S. Thesis, Purdue University, W. Lafayette, IN. 72 pp.

Shapiro, L.J., 1978: The vorticity budget of a composite African tropical wave disturbance. Mon. Wea. Rev., 106, 806-817.

Smith, P.J., 1970: An analysis of kinematic vertical motion. Mon. Wea. Rev., 99, 715-724.

Stevens, D.E., 1979: Vorticity, momentum and divergence budgets of synoptic-scale wave disturbances in the tropical eastern Atlantic. Mon. Wea. Rev., 107, 535-550.

Thompson, R.M., S.W. Payne, E.E. Recker and R.J. Reed, 1979: Structure and properties of synoptic-scale wave disturbances in the ITCZ of the eastern Atlantic. J. Atmos. Sci., 36, 53-72.

Torre, Y., C. Aspliden, M. Garstang and J. Cunningham, 1979: Mean tropical conditions over west Africa and eastern Atlantic ocean during GATE, Vol. I, kinematic analysis. University of Virginia, Dept. of Environmental Sciences, Charlottesville, VA.

Viltard, A. and P. dePelice, 1979: Statistical analysis of wind velocity in an easterly wave over western Africa. Mon. Wea. Rev., 107, 1320-1327.

Vincent, D.G., 1980: Large-scale mean state during phase III for GATE. I. Analysis of observed data. (Submitted for publication to Quart. J. Roy. Meteor. Soc.).

Vincent, D.G. and G.L. Scott, 1980: Large-scale mean state during phase III of GATE. II. Kinematics and energetics of the wind field. (Submitted for publication to Quart. J. Roy. Meteor. Soc.).

Vincent, D.G. and R.G. Waterman, 1979: Large-scale atmospheric conditions during the intensification of hurricane Carmen (1974). I. Temperature, moisture and kinematics. Mon. Wea. Rev., 107, 283-294.

APPENDIX

APPENDIX

a	radius of the earth
f	coriolis parameter
F_x	east-west component of friction
F_y	north-south component of friction
p	pressure
t	time
u	zonal component of velocity
v	meridional component of velocity
$\vec{V}$	horizontal wind vector on an isobaric surface
x	zonal direction
y	meridional direction
ζ	relative vorticity
ζ_a	absolute vorticity ($\zeta + f$)
Ω	angular velocity of the earth
ϕ	latitutde
ω	vertical velocity (dp/dt)
∂	partial derivative operator
∇_p	del operator on an isobaric surface

END

DATE
FILMED

1-81

DTIC